

# FRI Quantum Computing Stream

## Laboratory Manual

Charles Goode, Bernardo Oviedo, Khristina Pierce  
Advised by Jeremy Cook and Patrick Rall

August 22, 2018

## Contents

|          |  |           |
|----------|--|-----------|
| <b>1</b> | <b>Introduction</b>  | <b>2</b>  |
| <b>2</b> | <b>Lab Equipment</b>   | <b>2</b>  |
| <b>3</b> | <b>Alignment</b>   | <b>3</b>  |
| 3.1      | Free space . . . . .   | 3         |
| 3.2      | Power meter . . . . .  | 5         |
| 3.3      | FiberPort Collimation . . . . .                                    | 5         |
| 3.4      | Alignment of Two-Sided FiberPorts . . . . .                        | 7         |
| 3.5      | Alignment of Three-Sided FiberPorts with a Beam Splitter . . . . . | 7         |
| 3.6      | Polarization . . . . .   | 8         |
| 3.7      | Polarizers . . . . .   | 10        |
| 3.8      | Waveplates . . . . .   | 12        |
| 3.9      | Wave-plates - Characterization and Maintenance . . . . .           | 14        |
| 3.10     | Half Wave-Plate Experiment . . . . .                               | 15        |
| 3.11     | Malus' Law . . . . .   | 16        |
| 3.12     | Single Photon Detector (SPD) . . . . .                             | 17        |
| <b>4</b> | <b>Attenuation</b>   | <b>19</b> |
| 4.1      | Target Attenuation Range . . . . .                                 | 19        |
| 4.2      | Free Space Neutral Density Filters . . . . .                       | 19        |
| 4.3      | Variable Optical Attenuators . . . . .                             | 19        |
| 4.4      | Using Two Polarizers . . . . .                                     | 21        |
| <b>5</b> | <b>Quantum State Tomography</b>                                    | <b>22</b> |
| 5.1      | Tomography . . . . .   | 22        |
| 5.2      | Using the SPD . . . . .  | 25        |
| 5.3      | Setup . . . . .  | 25        |
| 5.4      | Mathematic Conventions and Conversions . . . . .                   | 26        |
| 5.5      | Fidelity . . . . .   | 27        |
| 5.6      | Mystery Tomography . . . . .                                       | 27        |
| 5.7      | Maximum Likelihood Estimation . . . . .                            | 27        |
| 5.8      | Error Analysis . . . . .   | 28        |
| 5.9      | Python Programs . . . . .  | 30        |
| 5.10     | Tomography using the Qubit SIC-POVM . . . . .                      | 31        |
| 5.11     | 6 vs 4 measurements . . . . .                                      | 33        |
| 5.12     | Mixed State Preparation and QST . . . . .                          | 33        |
| 5.13     | Automated QST . . . . .  | 33        |
| 5.14     | Mixed State Automated QST . . . . .                                | 37        |

# 1 Introduction

The purpose of this manual is to document the work done in the 2018 summer lab of the FRI Quantum Computing Stream and to help future students in this summer course be more efficient. The main project we focused on was performing and analyzing various forms of Quantum State Tomography. We passed a 785 nm laser through fiber optic cables for each of our QST set-ups. We first prepare a general state of a qubit using polarized light, which contains the same degrees of freedom as a qubit. We then set up a series of polarizers, wave-plates, polarizing beam splitters, and photon detectors to make measurements and reconstruct the initial quantum state (a density matrix).

## 2 Lab Equipment

### Polarizers

- (1) FBR-LPNIR - Rotating Linear Polarizer Module, 650 - 2000 nm - <https://www.thorlabs.com/thorproduct.cfm?partnumber=FBR-LPNIR>
- (1) LPNIRE050-B - Ø1/2" Linear Polarizer with N-BK7 Windows, 600-1100 nm - <https://www.thorlabs.com/thorproduct.cfm?partnumber=LPNIRE050-B>
- (1) FiberBench Linear Polarizer Module (but no polarizer)

### λ/4 Wave Plates

- (4) Achromatic 1/4 Wave Plate Module 700-1200nm - <https://www.thorlabs.com/thorproduct.cfm?partnumber=FBR-AQ2>
- (1) 1" mounted LCP 1/4 Wave Plate 780nm - <https://www.thorlabs.com/thorproduct.cfm?partnumber=WPQ10ME-780>

### λ/2 Wave Plates

- (2) Achromatic 1/2 Wave Plate Module 700-1200nm - <https://www.thorlabs.com/thorproduct.cfm?partnumber=FBR-AQ2>
- (1) 1" mounted LCP 1/2 wave plate, 780nm - <https://www.thorlabs.com/thorproduct.cfm?partnumber=WPH10ME-780>

### Beamsplitters

- (1) FBT-50NIR - 50:50 Fiberbench Beamsplitter Module, 600 - 1700 nm - <https://www.thorlabs.com/thorproduct.cfm?partnumber=FBT-50NIR>

### FiberPorts

- (3) PAF-X-2-B - FiberPort, FC/PC & FC/APC, f=2.0 mm, 600 - 1050 nm - <https://www.thorlabs.com/thorproduct.cfm?partnumber=PAF-X-2-B#ad-image-0>
- (2) PAF-X-4-B - FiberPort, FC/PC & FC/APC, f=2.0 mm, 600 - 1050 nm - <https://www.thorlabs.com/thorproduct.cfm?partnumber=PAF-X-2-B#ad-image-0>

### Collimators

- (1) Adjustable FC/PC or APC Collimator 650 - 1050 nm, EFL 4.6mm
- (1) Adjustable FC/PC or APC Collimator 650 - 1050 nm, EFL 7.5mm
- (1) Fiber Collimation Package, 633nm, f = 10.99 mm, FC/PC

### Uncatagorized:

- (2) 25.4mm Dia. Round Silver Mirror 3.2mm Thick
- (2) K10CR1/M - Motorized Rotation Mount for Ø1" Optics, Stepper Motor, Metric

For manuals, visit [www.thorlabs.com/manuals](https://www.thorlabs.com/manuals).

## 3 Alignment

### 3.1 Free space

The goal of free space alignment is to have the laser emit from a collimator and be re-collimated by a receiving collimator. The laser can then be attenuated with free space neutral density filters. Before setting up the alignment:

- Make sure the collimators are tightly screwed into their stands so that the laser will be as close to parallel with the table as possible.
- Connect the laser to the emitting collimator via optic fiber. You will have to twist the optic fiber until the key inserts into the notch before screwing it in.

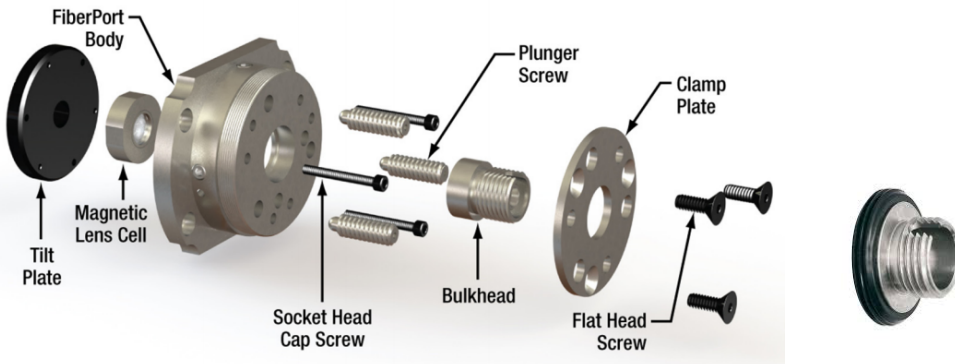


Figure 1: Screwing optic fibers into their ports can be tricky. Note that there is a small notch in the port.

- Verify/check the height of the laser by making a "target." Tape a white index card to a magnetic stand. Place it close to the collimator emitting the laser and mark the height with a pen. Slide the target far away from the collimator and make sure the laser is hitting the same height. This should be checked for both collimators

Moving an index card along the length of the beam, you should observe either a collimated beam, diverging beam, or converging beam.

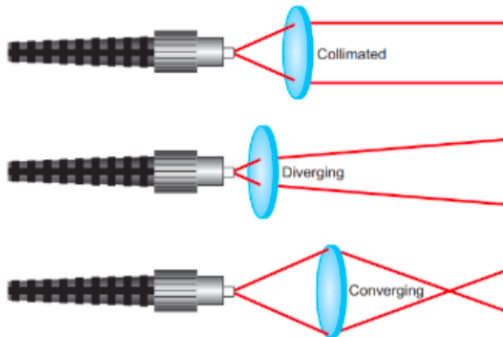


Figure 2: Three lens positions: collimated, diverging, and converging.

To allow for precise alignment adjustments, you will need to use mirrors. The knobs on the mirrors make smaller adjustments than you could do by hand if you just had the collimators directly in line with each other.

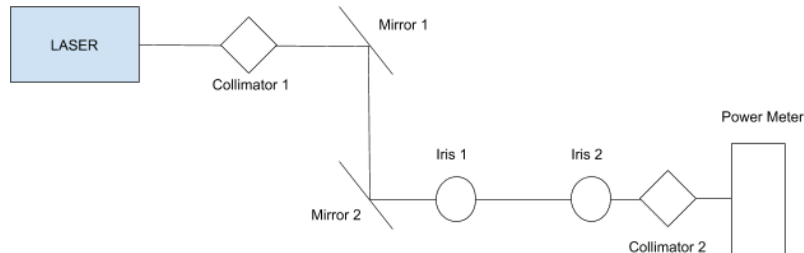


Figure 3: Diagram of a free space alignment.

The configuration pictured above worked best for us. To set it up:

1. Place the first mirror at least 6 inches away from the emitting collimator, directly in line with it. Use a white index card to make sure the laser is hitting the center of the mirror.
2. Angle the first mirror so that the laser is reflected perpendicular to its original direction.
3. Place the second mirror about 6 inches from the first, also angled so that the laser hits the center of the mirror and is reflected 90 degrees.
4. Place the receiving collimator about 6 inches from the second mirror, directly in line with it.

You should test the that the laser is hitting the center of the mirrors and the final collimator from both directions. This means you should switch the optic fibers so that the first collimator is now receiving the laser and the second collimator is emitting it. To avoid accidentally turning the collimators when switching optic fibers, the laser, collimators, and power meter can be connected to a mating sleeve.



Figure 4: Mating ports will allow you to switch the direction of the laser as often as needed without risking changes to the alignment.

Irises can help you keep track of the exact path the laser should take between components.



Figure 5: Irises.

To use the irises:

1. Between either collimator 1 and mirror 1 or collimator 2 and mirror 2, place two irises evenly spaced from each other, the mirror, and the collimator.

2. Pass the laser through the collimator closest to the irises, making sure the laser is hitting the centers of the mirrors and the lens of the receiving collimator as precisely as possible with a white index card.
3. Place the target behind the first iris and adjust it until you can close it almost all the way and still get the laser through. Repeat this placing the target after the second iris.
4. Open the irises just enough to not truncate the laser beam. The irises are now pin-pointing the exact spots the laser should be passing through from both directions.
5. Switch the direction of the laser and and adjust so that it can pass through the irises. You will likely see the beam hitting the edge of the iris and you can use this visual cue to make sure you adjust in the right direction.

Once the alignment is as precise as you can get it (hitting the exact center of the lens of the receiving collimator) from both directions, connect your receiving collimator to the power meter. If the laser is aligned, there will be a definite difference in the reading on the power meter when you block the laser for a few seconds. You can now make microscopic adjustments with the knobs on the mirrors while watching the power meter to maximize the power output of your alignment. This should also be done from both directions.

### **3.2 Power meter**

The lab's power meter measures from a hundredth of a nanowatt to around 2.5 miliwatts. This upper bound can be increased by sliding on the ND3 attenuator (reducing the power by a factor of 1000) that is built in to the detection strip. To measure the power from the laser:

1. Plug the fiber optic cable with the laser into a collimator screwed into a free space ring-shaped component holder.
2. Position this collimator and the detection strip of the power meter so that the beam hits the detection strip. The collimator ought to be close to the detection strip; approximately 1 cm apart.
3. Eyeballing at first, adjust the angle of the collimator so the beam should hit perpendicular to the plane of the detection strip.
4. With the power meter readout device attached and powered on, make slight adjustments searching for a maximum readout.
5. Lock every component in place tightly.
6. To reduce a constant in the readout due to ambient/environmental light, construct a cardboard cabin to house the power meter and collimator. Use ours if still available.

### **3.3 FiberPort Collimation**

FiberPort is a ThorLabs unique product that passes laser light into a short length of free-space and re-collimates it.



Figure 6: Two-Sided FiberPort.

Before aligning the fiberports, the sides of the port must be properly collimated. To collimate the fiberports:

1. Plug the fiber optic cable containing the laser into one side of the fiber bench.
2. Remove any obstruction in the laser's path for 1-3 feet (requires removing the opposing side).
3. Starting close to the laser, use a surface (business card or sticky note) to catch (sometimes easier to view through a phone's camera lens) the beam coming out of the collimator. Adjust the 3 z-screws on the face of the collimation component so the beam becomes more point-like (less diffuse or blurry).
4. Make only a slight improvement before moving to the next screws iteratively so as to reach a collimation with roughly equal use of each screw.
5. Move the viewing surface out one foot further from the collimator and repeat the process up to about three feet.

The manual for the PAF-X-2-B from ThorLabs is a good resource to understand how the fiberports work.: [https://drive.google.com/file/d/1-\\_0h5awx4WDb01S0wY7Gus0KfLiEoDWr/view?usp=sharing](https://drive.google.com/file/d/1-_0h5awx4WDb01S0wY7Gus0KfLiEoDWr/view?usp=sharing)

Chapter 4 is useful for collimating a beam, and Chapter 6 is useful for FiberPort alignment.

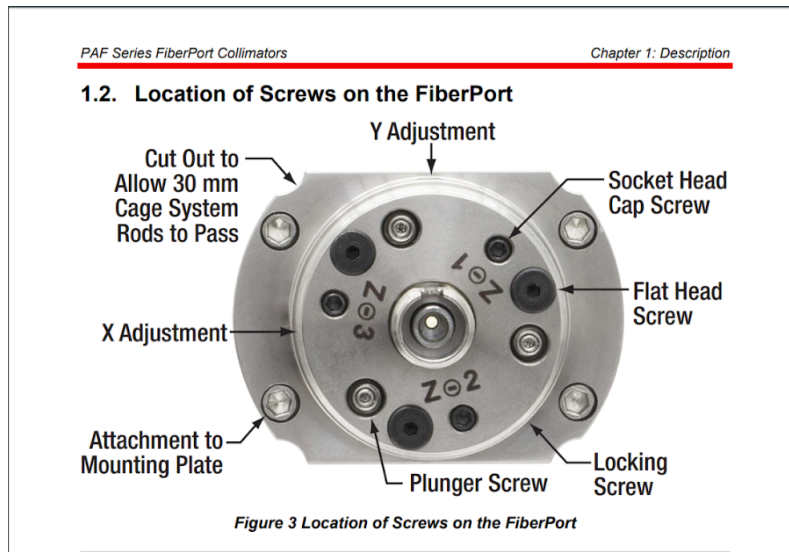


Figure 7: Location of the FiberPort screws. This is a page from the manual for the PAF-X-2-B from ThorLabs.

### **3.4 Alignment of Two-Sided FiberPorts**

After collimating both sides and with the laser plugged into one side and the power meter in the other, the fiberport can be aligned.

1. Adjust the x and y screws until the beam appears to go directly into the lens in the other collimator. It may be useful to place a viewing surface between the beam and the collimator to see the position of the incident beam.
2. Looking into the lens in the collimator, the beam should not hit the metallic side of the hole. When properly aligned, the beam should not be visible anywhere on the collimator except the lens (which is not reflective, so you shouldn't see anything).
3. Adjust the z-screws on both collimators to maximize the power output. For each screw, turn it in both directions so that you know which direction increases output the most. Once you cannot get any more power output from turning that screw, move on to the next screws iteratively, so that the three screws are adjusted roughly by the same amount.
4. Once power is maximized on that collimator, start adjusting the screws on the other in the same fashion.
5. Repeat this process of maximizing each screw and each collimator until no further progress can be made. The 2-sided fiber benches can typically be aligned to a power difference only 1 order of magnitude compared to the raw laser.

Note: The 2-sided fiber benches have different collimator models: -X-4-B and -X-2-B. Do not mix these up; aligning collimators of differing model will never be as successful.

### **3.5 Alignment of Three-Sided FiberPorts with a Beam Splitter**

1. After collimating each side, align the two sides facing each other as you would a 2-sided fiber bench.
2. With the 50/50 beam splitter in place, plug the laser into the third side and the power meter into the output side.
3. Ensure the beam splitter mount is level with the fiber bench. This can be adjusted with a few screws on the component. (Refer to the ThorLabs documentation for details.)
4. Make sure the beam splitter is oriented so that the third side and one of the parallel sides act as inputs with half of each of their beams entering the remaining parallel side (the output).
5. Make adjustments only to the third side's screws in the manner of 2 sided alignment. Once the power is maximized, record it for comparison with the other input side.
6. Switch the laser to the other input side and adjust to maximize power output and to balance the two inputs' contribution to the power output. This will require switching the laser frequently.
7. It may be helpful to adjust the output side z-screws, but do so with caution. This may cause drastic variance in the alignment of the two inputs with the output.

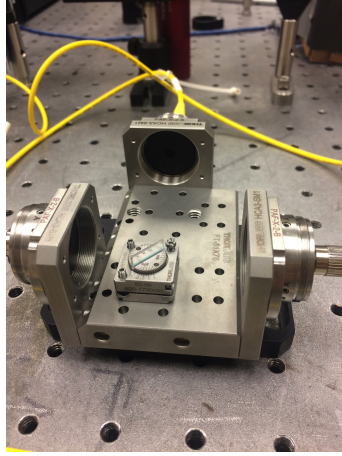


Figure 8: This is a 3-sided FiberPort with a beam-splitter positioned so that the left side is the output and the top and right sides are the inputs

Note: altering the plane of the beam splitter mount usually causes heavy fluctuation in output. It seems best to avoid this degree of freedom.

### 3.6 Polarization

All electromagnetic radiation follows Maxwell's equations of electromagnetism, and one such solution to Maxwell's equations is

$$\vec{E} = E_0 \hat{\mathbf{e}} \cos(\omega t - kz + \phi_0), \quad (1)$$

$$\vec{B} = B_0 \hat{\mathbf{b}} \cos(\omega t - kz + \phi_0). \quad (2)$$

where the vector  $\hat{\mathbf{e}}$  is a unit vector that points in the direction of the electric field, the vector  $\hat{\mathbf{b}}$  is a unit vector that points in the direction of the magnetic field,  $E_0$  is the amplitude of the electric field,  $B_0$  is the amplitude of the magnetic field,  $\omega$  is the frequency,  $k$  is the wave vector,  $\phi_0$  is the phase, and  $z$  is the direction of propagation. Maxwell's equations place additional constraints on this solution. The first is that the wave (in vacuum) must travel at the speed of light,  $\omega = ck$ . Secondly, the magnitude of the magnetic field must be equal to  $E_0/c$ . Lastly, the electric field vector  $\hat{\mathbf{e}}$  and the magnetic field vector  $\hat{\mathbf{b}}$  must be orthogonal, and the direction of propagation of the wave is equal to their cross product, i.e.  $\hat{\mathbf{z}} = \hat{\mathbf{e}} \times \hat{\mathbf{b}}$ . This particular solution is called an electromagnetic plane wave that propagates in the  $\hat{\mathbf{z}}$  direction, where we take  $\hat{\mathbf{k}} \equiv \hat{\mathbf{z}}$ .

The shape that the  $\hat{\mathbf{e}}$  vector carves out as time goes on is called the **polarization** of the light in question, and thus we will only focus on the oscillating electric field of light. Since  $\hat{\mathbf{e}}$  is a vector in the plane perpendicular to  $\hat{\mathbf{k}}$ , we can choose to write it in any basis. Assuming that our electromagnetic wave propagates in the  $\hat{\mathbf{z}}$  direction, we can choose to represent  $\hat{\mathbf{e}}$  in the conventional  $\{\hat{\mathbf{x}}, \hat{\mathbf{y}}\}$  basis. Furthermore since Maxwell's equations obey superposition, the most general form of equation (1) can be written as

$$\hat{E} = E_{01} \hat{\mathbf{x}} \cos(\omega t - kz + \phi_1) + E_{02} \hat{\mathbf{y}} \cos(\omega t - kz + \phi_2). \quad (3)$$

There are 4 free parameters in equation (3), which determine the polarization of the electric field. In the case  $\phi_1 = \phi_2 \equiv \phi_0$  we have **linear polarization**, as shown in Figure 9. In this case we have

$$\hat{E} = (E_{01} \hat{\mathbf{x}} + E_{02} \hat{\mathbf{y}}) \cos(\omega t - kz + \phi_0). \quad (4)$$

Or we can write the electric field as

$$\hat{E} = E_0 \hat{\mathbf{e}} \cos(\omega t - kz + \phi_0), \quad (5)$$

where

$$E_0 = \sqrt{E_{01}^2 + E_{02}^2}, \quad (6)$$

and

$$\hat{\mathbf{e}} = \frac{E_{01}}{E_0} \hat{\mathbf{x}} + \frac{E_{02}}{E_0} \hat{\mathbf{y}}. \quad (7)$$

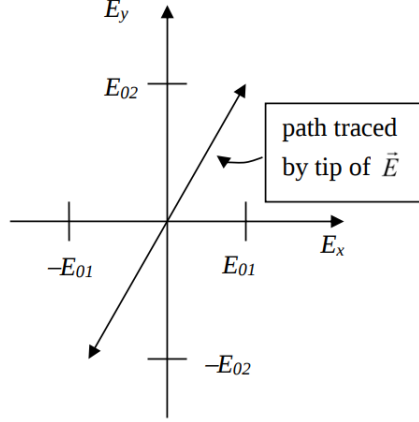


Figure 9: Linearly polarized light traced by the tip of the  $\hat{\mathbf{e}}$  vector. Image source: [7].

If  $\phi_0 = \phi_1 = \phi_2 \pm \pi/2$  and  $E_{01} = E_{02}$  then we have **circularly polarized** light. We can write the field as

$$\hat{E} = \frac{E_0}{\sqrt{2}} (\hat{\mathbf{x}} \cos(\omega t - kz + \phi_0) \pm \hat{\mathbf{y}} \sin(\omega t - kz + \phi_0)). \quad (8)$$

There are two possible directions of rotation of the  $\vec{E}$ -field vector, which are called *left-circular polarization* and *right-circular polarization*.

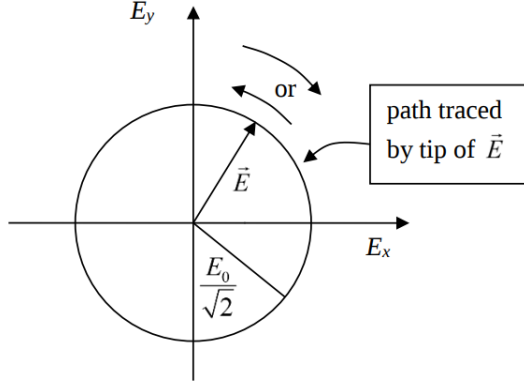


Figure 10: Circularly polarized light traced by the tip of the  $\hat{\mathbf{e}}$  vector. Image source: [7].

In the most general case, we have **elliptically polarized** light so long as  $\phi_1 \neq \phi_2$ ,  $\phi_1 \neq \phi_2 \pm \pi/2$ , and  $E_{01} \neq E_{02}$ . The equation for the electric field is written the same as equation (3).

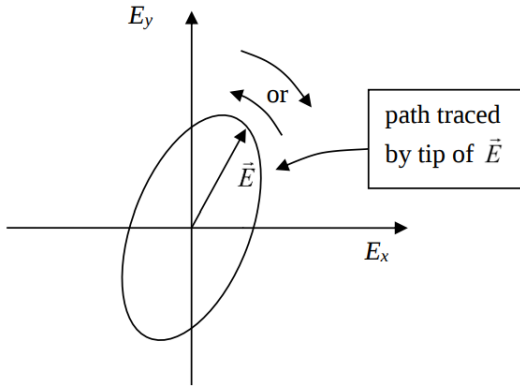


Figure 11: Elliptically polarized light traced by the tip of the  $\hat{\mathbf{e}}$  vector. Image source: [7].

Natural light is often unpolarized, or decoherent. Coherent light is light with a definite polarization, whereas decoherent light has a random or non-consistent polarization. Decoherent polarization occurs whenever the source of radiation is composed of radiators that have no net orientation or handedness. Coherent linearly polarized radiation can be produced with polarizers. For microwaves and infrared radiation, the wire-grid polarizer can be used, which consists of a set of parallel metal wires. When an electromagnetic wave hits the polarizer, the component of the field that is parallel to the wires drives an oscillating current in them. Energy is dissipated due to the electrical resistance of the wires, and this absorbs a lot of the energy from the polarization component parallel to the wire. However due to imperfections in manufacturing the light that leaves the polarizer isn't purely polarized, but very close to it. The light that is polarized in the direction perpendicular to the metal wires are not absorbed, and this polarization state passes through. A diagram of a wire grid polarizer is shown in Figure 12.

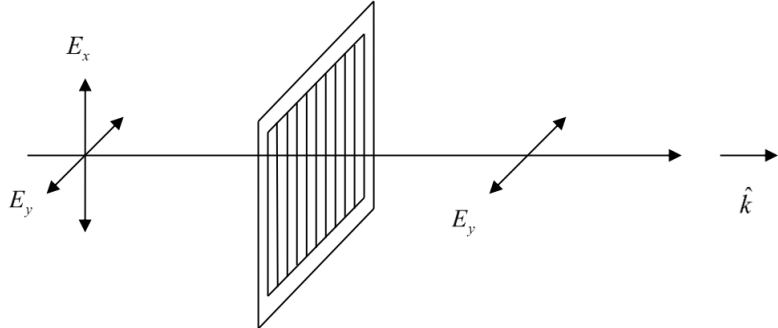


Figure 12: Wire grid polarizer that only permits horizontal polarization.

### 3.7 Polarizers

It would seem that the behavior of linear polarizer components made for fiberports heavily depends on the fiberport alignment. Furthermore, the power output is not symmetric about 180 degree turns in the polarizers. This is likely due to imperfections in the components and/or a polarization dependence in the fiberport collimators. We conducted a series of component characterization experiments to find ways of compensating for irregular, asymmetric polarizers.

The two polarizers in the lab are not interchangeable. They have maximum power outputs at different angles and have different asymmetries. Therefore, we differentiate them by naming them "Polarizer 1" and "Polarizer 2".



Figure 13: Polarizer 1 has the white reference line on the surface of polarizer. This line can be trusted since it is affixed to the lens itself. The angle dial on the polarizer mount however may not correspond to this line over time. There is a ring holding the lens to the component that can be tightened and loosened. Adjust as seen fit (noting the relation of the reference line to the angles on the dial) and screw tight the ring-shaped holder.

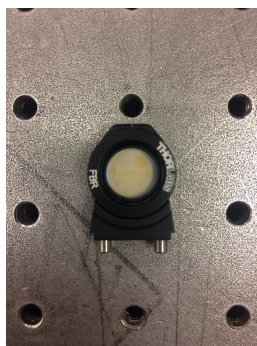


Figure 14: Polarizer 2 has no reference line. Adjust the ring holding the lens as needed and screw tight into the ring-shaped holder.

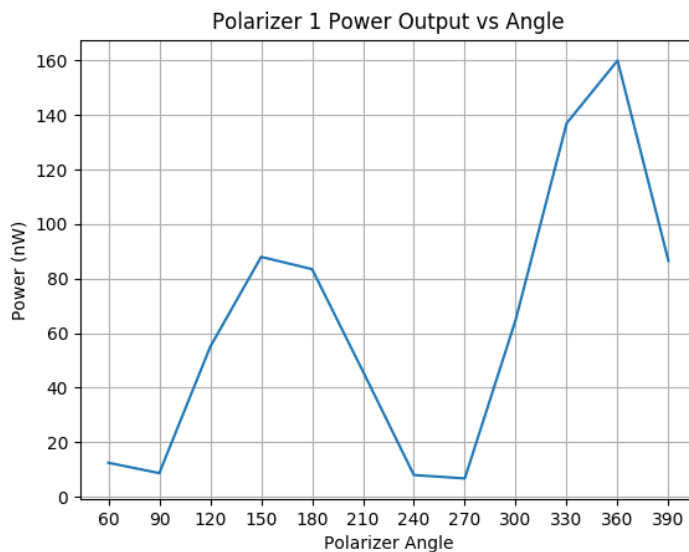


Figure 15: Notice that the shape of the above data is sinusoidal as expected, but that the power outputs are not consistent with 180 degree rotations.

The solution to the asymmetry problem that yields the highest QST fidelities is to average the power outputs at the angle and  $180^\circ$  away from it. This doubles the number of measurements

but does not require any extra time spent “re-collimating.” This method works because of an important observation: the issue is with relative amplitude/intensity not with the locations of the values. Essentially, the local extrema are more or less in the right place by angle but the power output relative to each other is the issue. Averaging the two angles on the polarizer of the same polarization normalizes the difference.

If this solution does not work for some unforeseen reason, a secondary solution is to re-collimate the fiberport after inserting the polarizers as follows:

1. Place two linear polarizers into the fiber bench to be realigned. Typically, polarizer 1 (P1) goes first (the laser passes through it first).
2. Pick a particular polarization on the first polarizer; the useful choices are horizontal, vertical, diagonal, and anti-diagonal.
3. When the second polarizer is turned to a maximum, note its angle and power output and move  $180^\circ$ . The power output ought to be equal with that of the previous angle, but it likely is not.
4. Going back and forth between these two angles, adjust the z-screws until the two angles have roughly equal power outputs.
5. The maximum power output angles have now likely changed. Find the new angle with max power and adjust the z-screws to equalize the power output between it and the angle  $180^\circ$  from it. Repeat this step until the two maximums occur  $180^\circ$  degrees apart and the power outputs at these angles are equal.
6. Check that the angles orthogonal to the maximums are minimums. If not, attempt to balance them and begin again on the maximums.
7. Ensure the angles for diagonal and anti-diagonal behave properly as well.
8. When satisfied, record the values on P2 for each of the polarization states.

Most calibration processes in this lab are iterative.

### 3.8 Waveplates

Light travels the fastest in a pure vacuum and travels slower through other mediums, such as transparent materials. The fact that the speed of light in a transparent material travels slower than the speed of light in a vacuum is called **refraction**. The *index of refraction* of a material is the factor by which the speed is reduced,

$$n = \frac{c}{v}. \quad (9)$$

A **birefringent** material has a different index of refraction depending on the polarization of the incident light. This occurs because the material’s bound electrons vibrate more strongly in response to an electric field of one polarization than in response to another polarization. It is of this (transparent) material that waveplates are made.

A waveplate is a thin plate of transparent birefringent material cut in such a way that there are two special axes in the plane of the plate that are perpendicular to each other: the *fast axis* and the *slow axis*. If light shining through the waveplate is linearly polarized parallel to the fast axis it will experience an index of refraction  $n_f$ . If light shining through the waveplate is linearly polarized parallel to the slow axis it will experience an index of refraction  $n_s$ . The waveplate is transparent, so theoretically light going through a waveplate suffers no loss of intensity.

The purpose of a waveplate is to create a relative difference between the phases of perpendicular components of the electric field. The component of the electric field parallel to the fast axis will experience a phase shift  $\Delta\phi_f$  relative to light in vacuum. Similarly the component of the electric field parallel to the slow axis will experience a phase shift  $\Delta\phi_s$  relative to light in vacuum. To calculate what these phase shifts are, first calculate how much longer the light going through the fast and slow axis are inside the waveplate length  $b$  compared to that of light in vacuum. Consider the experimental setup shown in Figure 16.

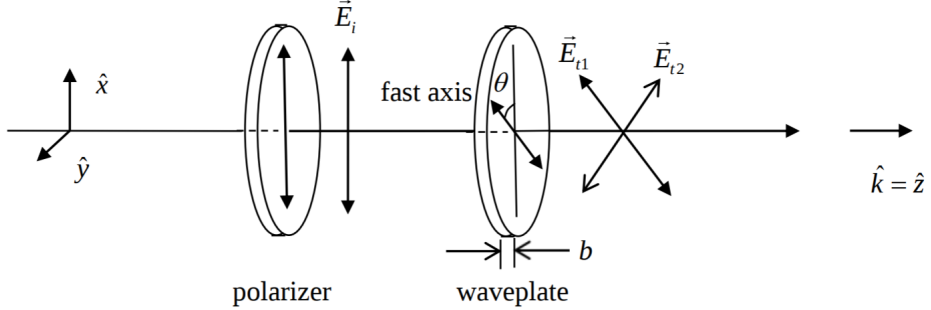


Figure 16: Unpolarized light becoming linearly polarized along the  $\hat{x}$  axis, and then going through a waveplate at an angle  $\theta$  with respect to the  $\hat{x}$  axis.

We start off with an electric field with no phase (for simplicity), which then becomes polarized along the  $\hat{x}$  axis:

$$\vec{E} = E_i \hat{x} \cos(\omega t - kz). \quad (10)$$

We employ the same change of basis to the basis  $\{\hat{e}_1, \hat{e}_2\}$  as we did for Malus' law,  $\hat{x} = \cos(\theta)\hat{e}_1 + \sin(\theta)\hat{e}_2$  so that our electric field is now

$$\vec{E} = (E_i \cos(\theta)\hat{e}_1 + E_i \sin(\theta)\hat{e}_2) \cos(\omega t - kz) = (E_{t1}\hat{e}_1 + E_{t2}\hat{e}_2) \cos(\omega t - kz). \quad (11)$$

Since solutions to Maxwell's equations obey superposition we can analyze the relative phase shift that will occur to each of these components and then sum the equation back together for the final solution. The relative phase shift along the fast-axis ( $\hat{e}_1$ ) with respect to a wave in vacuum is equal to the difference in time it takes for the light to travel through the waveplate  $\Delta t_f$  times the angular frequency of the wave  $\omega$ :

$$\Delta\phi_f = \Delta t_f \omega. \quad (12)$$

Distance equals rate times time, so the time it takes for light in vacuum to travel a distance of  $b$  is equal to  $b/c$ . Along the fast axis the wave experiences an index of refraction  $n_f = c/v_f$ . Therefore the difference in time is equal to

$$\Delta t_f = \frac{bn_f}{c} - \frac{b}{c} = \frac{b}{c}(n_f - 1). \quad (13)$$

The angular frequency is  $\omega = 2\pi f$ , and  $c = \lambda f$ , so the relative phase shift is

$$\Delta\phi_f = \frac{2\pi b}{\lambda}(n_f - 1). \quad (14)$$

By the exact same argument, the relative phase shift along the slow axis is

$$\Delta\phi_s = \frac{2\pi b}{\lambda}(n_s - 1). \quad (15)$$

Therefore the resulting electric field is

$$\vec{E} = E_{t1}\hat{e}_1 \cos\left(\omega t - kz - \frac{2\pi b}{\lambda}(n_f - 1)\right) + E_{t2}\hat{e}_2 \cos\left(\omega t - kz - \frac{2\pi b}{\lambda}(n_s - 1)\right). \quad (16)$$

However what we really care about is the relative phase difference between the two components of the electric field,  $\Delta\phi = \Delta\phi_f - \Delta\phi_s$ . This quantity times  $\lambda/2\pi$  is called the *retardation* of the wave plate,

$$\text{Retardation} = b(n_f - n_s). \quad (17)$$

It is equal to the distance light would have to travel in vacuum to accumulate a phase difference of  $\Delta\phi$ . Retardations are often specified as a number of wavelengths at a given wavelength. For example, a waveplate with a retardation of "1/4 wave at 635 nm" would have a retardation of 635

$\text{nm}/4 = 158.8 \text{ nm}$ . A quarter-wave plate is a waveplate with  $1/4$  wave of retardation at a specific wavelength. Therefore the retardation is equal to  $\lambda/4$ , which means

$$\Delta\phi = \frac{2\pi b}{\lambda} (n_f - n_s) = \frac{2\pi \lambda}{\lambda} \frac{1}{4} = \frac{\pi}{2}. \quad (18)$$

By placing the fast axis at an angle of  $45^\circ$ , the amplitudes of the electric field components along the fast and slow axis will be equal, and linearly polarized light is turned into circularly polarized light. A half-wave plate has a retardation of  $1/2$  wave at a specific wavelength, i.e. they produce a phase difference of  $\Delta\phi = \pi$  between the fast and slow components of the electric field. Half-wave plates at an angle  $\theta$  can be used to rotate the polarization of a linearly polarized beam through an angle  $2\theta$ .

### 3.9 Wave-plates - Characterization and Maintenance

Before any characterization, ensure that the lenses (with their affixed white reference lines) are well tightened to the mounting component. Be careful to not touch a lens. In case of such an accident, use only special particle cleaner cloth intended for optics components to clean them.

To characterize a  $1/2$  (or “half”) wave-plate or a  $1/4$  (or “quarter”) wave-plate:

1. Place it between two polarizers at the same polarization, all in the fiberport.
2. Rotate the wave-plate incrementally over  $360^\circ$ , recording the power measured at each increment. Plot this against  $\frac{\sin(2\theta)+1}{2}$  for a half wave-plate or  $\frac{\cos(2\theta)+1}{2}$  for a quarter wave-plate.
3. Observe what constant shift in  $\theta$  fits the data to this function best. Record this shift and label the wave-plate.
4. For future use of the wave-plate, ensure that you adjust your angles for this constant.

Important notes:

- Take into account that an angle in the Bloch/Poincaré sphere is twice that of a real angle:  $\theta_B = 2\theta_R$ .
- If only a half wave-plate is used in a linearly polarized state it will maintain the state in the linear plane. In order to move to the circular or imaginary state a quarter wave-plate must be applied.
- A half wave-plate does a half turn on the Bloch sphere based on the axis of rotation and a quarter wave-plate does a quarter turn.
- For a half wave-plate the direction of the axis is irrelevant but in a quarter wave-plate it is important since it can take turn to different quadrants depending on the direction.

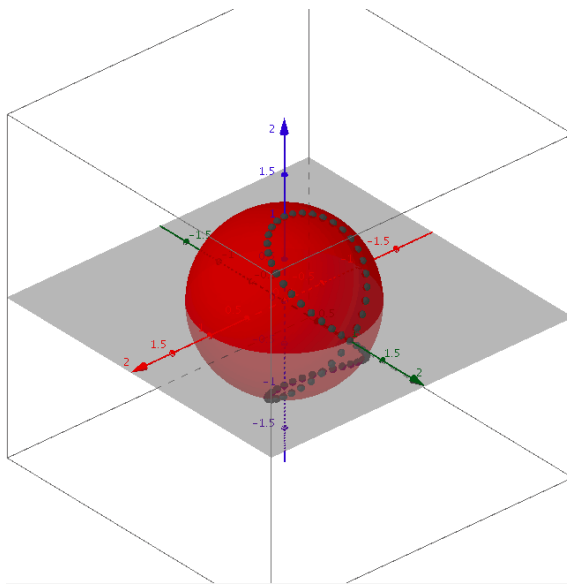


Figure 17: A 3-D graph on the Bloch sphere of a polarization state as the quarter wave-plate is rotated 360°.

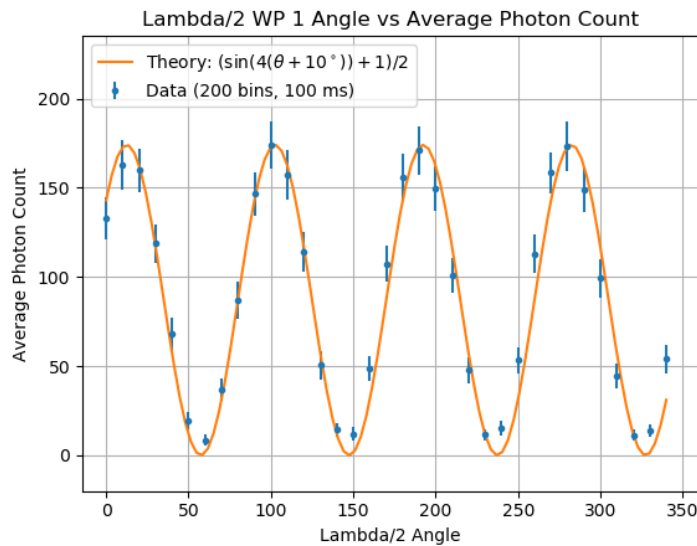


Figure 18: Our characterization of wave-plate 1.

### 3.10 Half Wave-Plate Experiment

This experiment confirms that a half wave-plate for a specific wavelength doubles the angle of polarization.

1. Place a linear polarizer, then half wave-plate, then another linear polarizer in the FiberPort.
2. With the first polarizer and half wave-plate at an arbitrary angle, maximize the power by rotating the second polarizer and record its angle.
3. Rotate the half wave-plate by some angles  $\theta_1$ ,  $\theta_2$ , and  $\theta_3$  and maximize the power output by rotating the second polarizer. Record the angles of the second polarizer when the power is at a maximum.

At what relative angles do you expect the second polarizer to maximize the power output? Do your angles match well with the theoretical predictions?

### 3.11 Malus' Law

Suppose that a linearly polarized electromagnetic wave propagates through two polarizers in sequence, the first vertically polarized, and the second polarized at an angle  $\theta$  with respect to the vertical, as shown in Figure 19. Suppose that the polarizers are ideal and transmit 100% of light that is polarized parallel to its polarization direction, and transmits 0% of light that is polarized perpendicular to its polarization direction. Let  $I_0$  be the intensity of light before the first polarizer, and let  $I_1$  be the intensity of light after the first polarizer. What we aim to find is the intensity of light after the second polarizer as a function of the angle  $\theta$  between the two polarizers, which we will call  $I_2$ .

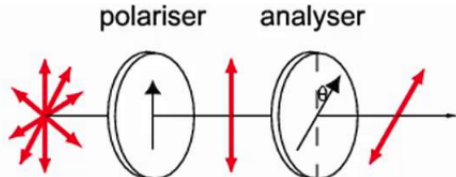


Figure 19: Unpolarized light passing through a vertical polarizer, and then another polarizer at an angle  $\theta$  with respect to the vertical. The intensity of light that emerges follows Malus' law.

Since the incoming light in the first stage of the apparatus is randomly polarized, we know that we will receive a 50% intensity loss, because the incident light has an equal chance to be horizontally polarized as it does vertically polarized, so  $I_1 = I_0/2$ . Next, to represent the electric field coming out of the first polarizer, we are free to choose any two perpendicular unit vectors in the plane. Let's choose the vector  $\hat{\mathbf{e}}_1$  which coincides with the transmission axis of the second polarizer. Pick another vector perpendicular to  $\hat{\mathbf{e}}_1$  such that  $\hat{\mathbf{e}}_1 \times \hat{\mathbf{e}}_2 = \hat{\mathbf{z}}$ . We can then write these vectors as

$$\hat{\mathbf{e}}_1 = \cos(\theta)\hat{\mathbf{x}} + \sin(\theta)\hat{\mathbf{y}} \quad (19)$$

$$\hat{\mathbf{e}}_2 = -\sin(\theta)\hat{\mathbf{x}} + \cos(\theta)\hat{\mathbf{y}}. \quad (20)$$

Rewriting  $\hat{\mathbf{x}}$  in terms of this new basis gives  $\hat{\mathbf{x}} = \cos(\theta)\hat{\mathbf{e}}_1 - \sin(\theta)\hat{\mathbf{e}}_2$ . The electric field after the first polarizer becomes

$$\vec{E} = E_0 \hat{\mathbf{x}} \cos(\omega t - kz + \phi) = E_0 (\cos(\theta)\hat{\mathbf{e}}_1 - \sin(\theta)\hat{\mathbf{e}}_2) \cos(\omega t - kz + \phi). \quad (21)$$

Then after we pass through the second polarizer, which is now conveniently projecting onto  $\hat{\mathbf{e}}_1$ , the electric field becomes

$$\vec{E} = E_0 \cos(\theta)\hat{\mathbf{e}}_1 \cos(\omega t - kz + \phi). \quad (22)$$

Since the intensity of light is proportional to the square of the amplitude, the intensity of the electric field is now reduced by a fraction of  $\cos^2(\theta)$ . Therefore the final intensity is  $I_2 = I_1 \cos^2(\theta)$ , or  $I_2 = I_0 \cos^2(\theta)/2$ . This is Malus' Law. The arrangement of the second polarizer with an adjustable relative angle provides an easy way to make an adjustable attenuator. It is useful to conduct an experiment to test Malus's Law and to verify that the lab polarizers are functioning properly.

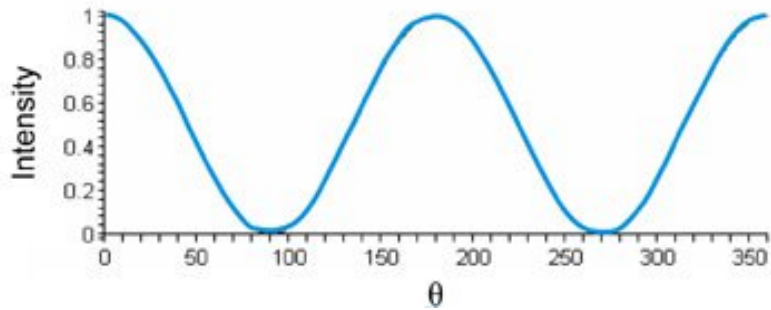


Figure 20: "Intensity" refers to the light after it has passed through P2 and " $\theta$ " refers to the angle P2 is at. With P1 and P2 in a fiberport, with P1 first, we rotated P2  $360^\circ$  and recorded the intensities. Theoretically, the intensity traces a  $\cos^2(\theta)$  path over a  $360^\circ$  rotation of P2. Additionally, the intensity is symmetric about  $180^\circ$ .

### 3.12 Single Photon Detector (SPD)



Figure 21: The above SPD is connected to a power source and a computer for data collection. The fiber optic cable, adjustable collimator, lens tube, and detection chip are in alignment and are properly collimated.

To connect a fiber optic cable containing the beam to the SPD, the cable must be plugged into the adjustable collimator, which in turn is affixed to a tube component that holds the collimator a specific distance from the SPD's detection chip and shelters this final free space component from ambient light.

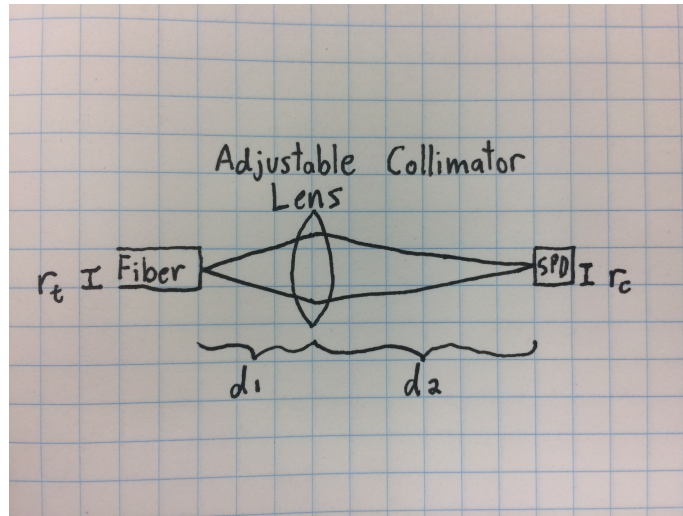


Figure 22: Diagram of the variables listed below.

There are 6 important values for proper collimation:

1.  $\lambda$ , the wavelength of the laser (785 nm)
2.  $d_1$ , the distance between the fiber's tip and collimator lens
3.  $d_2$ , the distance between the collimator lens and the SPD chip
4.  $r_t$ , the radius of the fiber's tip
5.  $r_c$ , the radius of the SPD's chip
6.  $f$ , the focal length adjustable collimator lens

$$z_{\{t,c\}} = \frac{\pi r_{\{t,c\}}^2}{\lambda}$$

Solve:

$$\frac{f(d_1 + iz_t)}{f - (d_1 + iz_t)} + d_2 = iz_c$$

for  $d_1, d_2$ .

Based on our measurements, calculations, and the two focal lengths of the adjustable collimators available, we created this table:

| $f$    | $d_1$   | $d_2$  |
|--------|---------|--------|
| 4.6 mm | 0.5 cm  | 2.7 cm |
| 7.5 mm | 0.89 cm | 4.6 cm |

There are two, different sized collimator tube mounts, so, when choosing which collimator to use by focal length, make sure the tube can give you enough control over  $d_2$ .

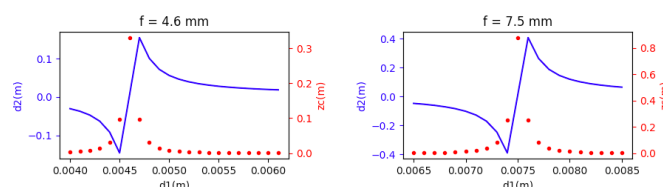


Figure 23: The above graphs display possible values for  $d_2$  and  $z_c$  as a function of  $d_1$  for the two adjustable collimators mentioned in the above table.

## 4 Attenuation

### 4.1 Target Attenuation Range

Attenuation is necessary because the SPD has a 22 MHz photon rate limit. If this count limit is exceeded, the chip could be damaged or destroyed.  $\text{PhotonRate} = \frac{\text{Power}\lambda}{hc}$ .

The 780nm raw laser has a power output of 10mW. The energy emitted per second is:

$$E_1 = Pt = (0.01W)(1s) = 0.01J$$

The energy per photon is given by:

$$E_\gamma = hf = \frac{hc}{\lambda}$$

The number of photons emitted per microsecond is approximated by:

$$N = \frac{E_1}{E_\gamma} = \frac{E_1\lambda}{hc} = \frac{(0.01J)(780 \times 10^{-9}m)}{(6.626 \times 10^{-34}Js)(3 \times 10^8m/s)} \cdot \frac{1s}{10^6 \mu s} \approx 3.92 \times 10^{10} \text{ photons}/\mu\text{sec}$$

The raw laser beam should be attenuated roughly 15 orders of magnitude; to the single photon regime.

- Note: Components such as free-space components and FiberPorts can attenuate the laser significantly on their own. Therefore, the factor of attenuation needed through variable and free-space neutral density filters is dependent on the type of experiment being performed and what components are a part of the system.

We have used two types of attenuation: free-space and variable.

- Free-space attenuation requires a free-space alignment but allows the use of neutral density filters.
- Variable attenuation allows for attenuation without free-space components. This is preferable because free-space alignments can be time consuming and tricky.

### 4.2 Free Space Neutral Density Filters

To protect the SPD detector chip, always start with at least an ND4 filter if unsure about the factor of attenuation needed. The number on the filter tells you the order by which it is attenuated. E.g. an ND3 will attenuate it by a factor of  $10^{-3}$ .

- When switching filters, make sure the laser is turned off so that the full power never fries the SPD.
- Generally, when the laser is going through only the free space attenuation and one fiberport use an ND4.
- Each time a new component is added (especially FiberPorts and beam splitters) there will be a higher factor of attenuation from the components and the alignment. Therefore, the more components in the system, the less free space attenuation is needed.
- If unsure that the neutral density filters in the system are enough attenuation, connect it to the power meter to make sure the beam is not too strong.

### 4.3 Variable Optical Attenuators

Variable Optical Attenuators give finer control on the attenuation of a beam than neutral density filters. This can be used to get the desired level of signal and to control the relative intensities of two lasers for mixed state preparation. There are two types of Knob Control sold by ThorLabs: Narrowband Variable Optical Attenuators (VOA's) and Dual Band VOA's.

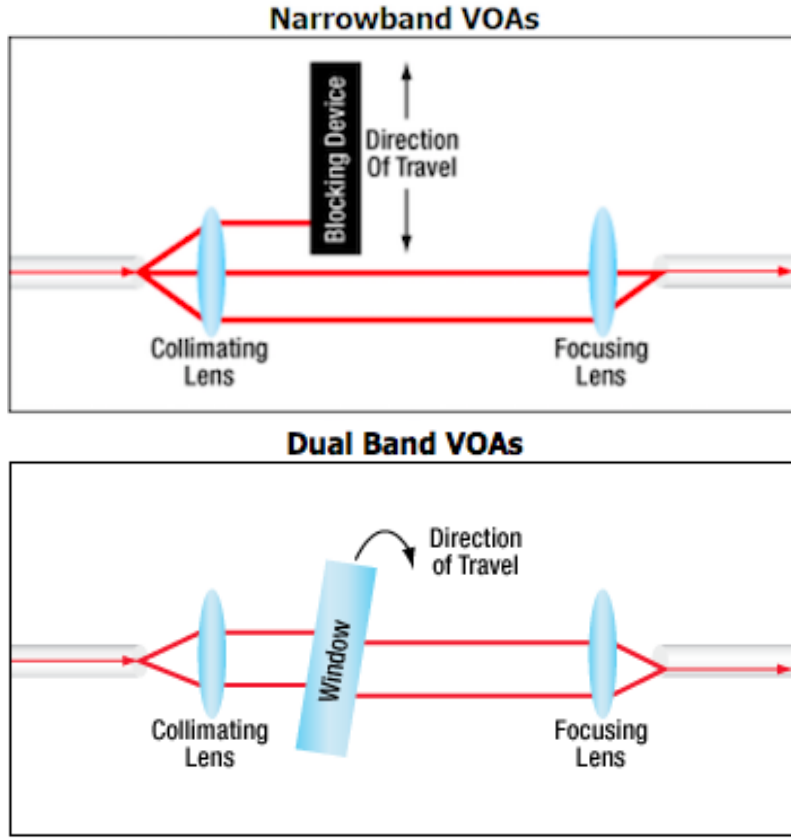


Figure 24: Narrowband VOA's work by simply blocking part of the laser beam while Dual Band VOA's use a window to change the path the laser beam travels which distorts the focus of the beam.

The orange variable attenuator in the lab is a Narrowband VOA. There is a small knob that allows precise adjustments to the attenuation. We characterized it by connecting it directly to the laser and SPD.

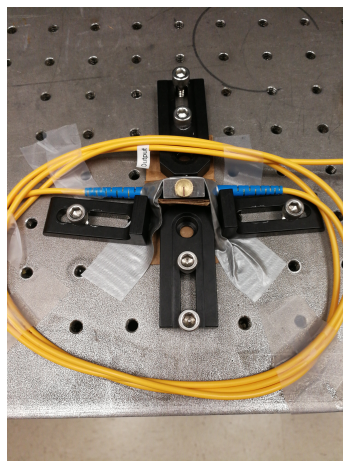


Figure 25: We had to make our own "mount" for the variable attenuator in the lab. The knob has been turned all the way clockwise and is completely blocking the laser.

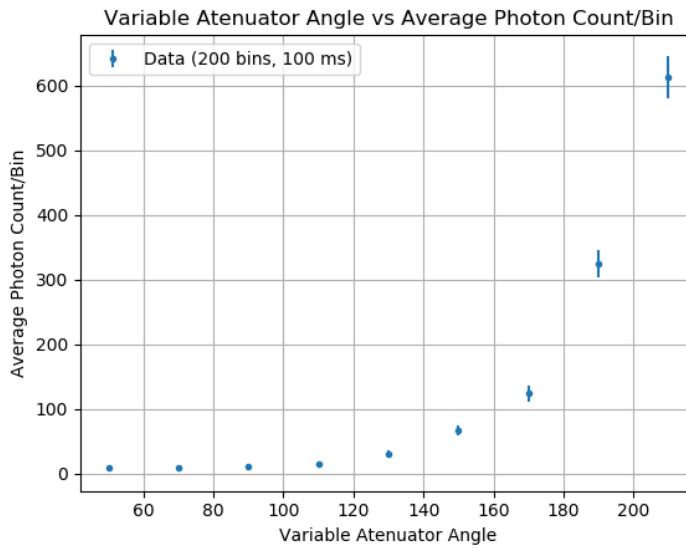


Figure 26: The average photon count per bin increases exponentially as the knob on the Narrowband VOA is turned counterclockwise past  $50^\circ$ .

To operate the Narrowband VOA:

- Turn the knob clockwise to attenuate and counterclockwise to increase power output.
- We have made a small mark on the circular knob to help keep track of how much attenuation each of the knob's positions provides. It is a line from the center to the edge.
- When the knob is screwed all the way clockwise, the line should be pointing “down” and the laser will be completely blocked.
- The knob can turn about  $50^\circ$  counterclockwise before reading any counts (except dark counts) on the SPD.
- After  $50^\circ$ , the photon count should double every 20 degree counterclockwise turn.
- Generally, when there is just one fiberport in the system, turn the knob 180 degrees from the completely off position and increase power from there if needed.
- Note: the more components are in the system, less attenuation will be needed and the knob will need to be turned further counterclockwise.

When turning the knob counterclockwise to increase the power output, monitor the average counts read by the SPD so that the chip is not damaged.

#### 4.4 Using Two Polarizers

Variable attenuation can theoretically also be achieved by using two linear polarizers and Malus’s Law. When completely plane polarized light is incident on the analyzer, the intensity of the light transmitted by the analyzer is directly proportional to the square of the cosine of angle between the transmission axes of the analyzer and the polarizer:

$$I_2 = I_1 \cos^2(\theta)$$

To attenuate via Malus’s Law:

1. Place two linear polarizers on a fiberport and lock the angle of the first one.
2. Move the relative angle of the second polarizer until the desired intensity is obtained and lock the angle of the second polarizer.

To read the intensity use the power meter since depending on your setup, it could be dangerous to read it from the SPD.

## 5 Quantum State Tomography

### 5.1 Tomography

The general principle behind quantum state tomography is that by repeatedly performing different measurements on quantum systems described by identical density matrices, frequency counts can be used to infer probabilities, and these probabilities can be combined with Born's rule to determine a density matrix that fits the best with the observations. Quantum state tomography is applied on a source of systems to determine the quantum state of the source. Unlike a measurement on a single system, which determines the system's current state after the measurement (in general, the act of making a measurement alters the quantum state), quantum state tomography works to determine the state prior to the measurements. To begin, recall that any pure/mixed state can be written in terms of Pauli matrices:

$$\rho = \frac{1}{2}(\mathbf{I} \text{Tr}(\mathbf{I}\rho) + \mathbf{X} \text{Tr}(\mathbf{X}\rho) + \mathbf{Y} \text{Tr}(\mathbf{Y}\rho) + \mathbf{Z} \text{Tr}(\mathbf{Z}\rho)). \quad (23)$$

where the Pauli matrices are

$$\mathbf{X} = \begin{pmatrix} 0 & 1 \\ 1 & 0 \end{pmatrix}, \quad \mathbf{Y} = \begin{pmatrix} 0 & -i \\ i & 0 \end{pmatrix}, \quad \mathbf{Z} = \begin{pmatrix} 1 & 0 \\ 0 & -1 \end{pmatrix}. \quad (24)$$

The coefficients of the Pauli matrices in equation (23) are scalar expectation values. The expectation value of any observable of a system in a state  $|\psi\rangle$  (or more generally in a state  $\rho$ ) is given by

$$\langle \mathbf{A} \rangle = \langle \psi | \mathbf{A} | \psi \rangle = \text{Tr}(\mathbf{A} |\psi\rangle \langle \psi|) = \text{Tr}(\mathbf{A}\rho), \quad (25)$$

which can be measured in the lab. The density matrix is then

$$\rho = \frac{1}{2}(\mathbf{I} + \mathbf{X} \langle \mathbf{X} \rangle + \mathbf{Y} \langle \mathbf{Y} \rangle + \mathbf{Z} \langle \mathbf{Z} \rangle). \quad (26)$$

To measure the expectation values of  $\mathbf{X}$ ,  $\mathbf{Y}$ , and  $\mathbf{Z}$ , first remember that we can write these observables in terms of their eigenvectors:

$$\mathbf{X} = |D\rangle \langle D| - |A\rangle \langle A|, \quad (27)$$

$$\mathbf{Y} = |R\rangle \langle R| - |L\rangle \langle L|, \quad (28)$$

$$\mathbf{Z} = |H\rangle \langle H| - |V\rangle \langle V|. \quad (29)$$

If our qubit is prepared in the state  $|\psi\rangle$ , then the expectation value for  $\mathbf{X}$  is

$$\langle \mathbf{X} \rangle = \langle \psi | \mathbf{X} | \psi \rangle = \langle \psi | (|D\rangle \langle D| - |A\rangle \langle A|) | \psi \rangle = |\langle \psi | D \rangle|^2 - |\langle \psi | A \rangle|^2. \quad (30)$$

which according to the Born rule is the probability of observing  $|D\rangle$  minus the probability of observing  $|A\rangle$ :

$$\langle \mathbf{X} \rangle = \text{Pr}(|D\rangle) - \text{Pr}(|A\rangle). \quad (31)$$

It follows that for  $\mathbf{Y}$  and  $\mathbf{Z}$ ,

$$\langle \mathbf{Y} \rangle = \text{Pr}(|R\rangle) - \text{Pr}(|L\rangle), \quad (32)$$

$$\langle \mathbf{Z} \rangle = \text{Pr}(|H\rangle) - \text{Pr}(|V\rangle). \quad (33)$$

In order to measure the probability of a state  $|\phi\rangle$  with respect to its orthogonal state  $|\phi'\rangle$ , we can do either of the following two procedures:

(i) Measure the average number of counts per bin recorded by the APD for each  $|\phi\rangle$  and  $|\phi'\rangle$ , which we will call  $n_1$  and  $n_2$ . The probability of observing the state  $|\phi\rangle$  can then be approximated by

$$\text{Pr}(|\phi\rangle) \approx \frac{n_1}{n_1 + n_2}. \quad (34)$$

This is of course an approximation because in order to determine the actual probability we would need to take an infinite amount of measurements, which then by the law of large numbers would approach  $\text{Pr}(|\phi\rangle)$ .

(ii) Measure the average counts per bin of the signal, which is the intensity of input state without any measurement polarizers. The waveplates can be left in the experiment because they are transparent and do not reduce the intensity of light. We would then only need to measure the average counts per bin of one of the states ( $n$ ), and not it's orthogonal state, to determine the probability of that state:

$$\text{Pr}(|\phi\rangle) \approx \frac{n_1}{n_s}. \quad (35)$$

This is again only an approximation, and it's error must be accounted for.

As a simple example, let's prepare the pure state  $|H\rangle$ . As a density matrix, we can write this pure state as an outer product  $|H\rangle\langle H|$ ,

$$\rho = |H\rangle\langle H| = \begin{pmatrix} 1 & 0 \\ 0 & 0 \end{pmatrix}. \quad (36)$$

To verify this is the density matrix calculated after performing QST, we first calculate the probabilities of measuring each of the basis states. This can be done theoretically with Born's law:  $\text{Pr}(|\psi\rangle) = \langle\psi|\rho|\psi\rangle$ . As an example, the probability of observing the diagonal state is calculated as follows:

$$\text{Pr}(|D\rangle) = \langle D|\rho|D\rangle = \frac{1}{2} (1 \ 1) \begin{pmatrix} 1 & 0 \\ 0 & 0 \end{pmatrix} \begin{pmatrix} 1 \\ 1 \end{pmatrix} = 0.5. \quad (37)$$

In order to measure in all the necessary bases, we must use half and quarter wave plates to project onto these states. The unitary operators for quarter wave plates (Q) and half wave plates (H) at an angle  $\theta$  with respect to the horizontal are given below.

$$W_Q(\theta) = \begin{pmatrix} \cos^2(\theta) + i \sin^2(\theta) & \frac{1}{2}(1-i)\sin(2\theta) \\ \frac{1}{2}(1-i)\sin(2\theta) & \sin^2(\theta) + i \cos^2(\theta) \end{pmatrix}, \quad (38)$$

$$W_H(\theta) = \begin{pmatrix} \cos(2\theta) & \sin(2\theta) \\ \sin(2\theta) & -\cos(2\theta) \end{pmatrix}. \quad (39)$$

The states  $\{|H\rangle, |V\rangle, |D\rangle, |A\rangle, |R\rangle, |L\rangle\}$  must be projected onto our measurement polarizer, which will be in the state  $|H\rangle$ . For the general state  $|\phi\rangle$ , we first apply a quarter wave plate then a half wave plate:

$$W_H^\dagger(\theta_H) W_Q^\dagger(\theta_Q) |\phi\rangle = |H\rangle, \quad (40)$$

or equivalently we can think about this in the reverse direction. If we think about the light being propagated backwards from the measurement polarizer, then

$$|\phi\rangle = W_Q(\theta_Q) W_H(\theta_H) |H\rangle. \quad (41)$$

What's left is to solve for the angles  $\theta_H$  and  $\theta_Q$  that project the state  $|\phi\rangle$  onto  $|H\rangle$ . These are recorded below, assuming that a quarter wave plate is placed first, then a half waveplate, then a polarizer in the horizontal state.

| Basis       | $\theta_Q$ | $\theta_H$ |
|-------------|------------|------------|
| $ H\rangle$ | 0          | 0          |
| $ V\rangle$ | 0          | $\pi/4$    |
| $ D\rangle$ | $\pi/4$    | $\pi/8$    |
| $ A\rangle$ | $\pi/4$    | $-\pi/8$   |
| $ R\rangle$ | 0          | $\pi/8$    |
| $ L\rangle$ | 0          | $-\pi/8$   |

To prepare a general qubit state at an angle  $\theta$  and  $\phi$  on the Poincaré sphere, i.e.  $|\phi\rangle = \cos(\theta/2)|R\rangle + e^{i\phi}\sin(\theta/2)|L\rangle$ , the angles in the transformation  $|\phi\rangle = W_Q(\theta_Q) W_H(\theta_H) |H\rangle$  are

$$\theta_H = \frac{\phi - \theta + \pi/2}{4} \quad (42)$$

$$\theta_Q = \frac{\phi}{2} \quad (43)$$

and to measure  $W_H^\dagger(\theta_H)W_Q^\dagger(\theta_Q)|\phi\rangle = |H\rangle$ ,

$$\theta_H = \frac{\phi + \theta - \pi/2}{4} \quad (44)$$

$$\theta_Q = \frac{\phi}{2}. \quad (45)$$

The angles  $\theta_H$  and  $\theta_Q$  are the angles the fast axis of the waveplate must make with respect to horizontal (assuming that the waveplate has 360 degrees, hence the extra factor of two). The angles  $\theta$  and  $\phi$  are shown in Figure 27 below, except we take  $|0\rangle$  to be  $|R\rangle$  and  $|1\rangle$  to be  $|L\rangle$ .

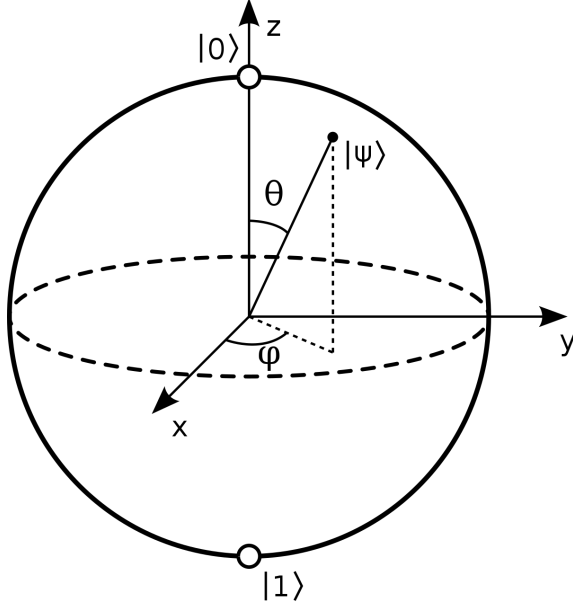


Figure 27: The Bloch sphere.

Visualize the waveplate transformations in Mathematica:

```

ClearAll;
input = {{1}, {0}};
quarter[x_] :=
  ConjugateTranspose[{{Cos[x]^2 +
    I*Sin[x]^2, (1/2) (1 - I) Sin[2*x]}, {(1/2) (1 - I) Sin[2*x],
    Sin[x]^2 + I*Cos[x]^2}}];
half[x_] := {{Cos[x]^2 - Sin[x]^2, Sin[2*x]}, {Sin[2*x],
  Sin[x]^2 - Cos[x]^2}};
getOutputRho[h_,
  q_] := (quarter[q].half[h].input).ConjugateTranspose[
  quarter[q].half[h].input];
getX[h_, q_] := getOutputRho[h, q][[2, 1]] + getOutputRho[h, q][[1, 2]];
getY[h_, q_] :=
  I (getOutputRho[h, q][[1, 2]] - getOutputRho[h, q][[2, 1]]);
getZ[h_, q_] :=
  getOutputRho[h, q][[1, 1]] - getOutputRho[h, q][[2, 2]];
Manipulate[
 Graphics3D[{Opacity[0.4], Sphere[], {EdgeForm[{Dashed, Red}],
  FaceForm[None], Cylinder[{{0, 0, -.001}, {0, 0, .001}}]}, {Dashed,
  Line[{{0, 0, 0}, {1, 0, 0}}], {Dashed,
  Line[{{0, 0, 0}, {0, 1, 0}}]}, {Dashed,
  Line[{{0, 0, 0}, {0, 0, 1}}]}, Text[Style["|H\[RightAngleBracket]", 14], {0, 0, 1.3}],
  Text[Style["|V\[RightAngleBracket]", 14], {0, 0, -1.3}],
  Text[Style["|D\[RightAngleBracket]", 14], {1.3, 0, 0}]},
  PlotRange->{{-.5, 1.5}, {-1.5, 1.5}, {-1.5, 1.5}}]
  
```

```

Text[Style["|A\[RightAngleBracket]", 14], {-1.3, 0, 0}],
Text[Style["|R\[RightAngleBracket]", 14], {0, 1.3, 0}],
Text[Style["|L\[RightAngleBracket]", 14], {0, -1.3, 0}],
Text[Style["r", 18, Red],
.5 {getX[halfAngle*\[Pi]/180, quarterAngle*\[Pi]/180],
getY[halfAngle*\[Pi]/180, quarterAngle*\[Pi]/180],
getZ[halfAngle*\[Pi]/180, quarterAngle*\[Pi]/180]}, {Red,
Arrow[{0, 0,
0}, {getX[halfAngle*\[Pi]/180, quarterAngle*\[Pi]/180],
getY[halfAngle*\[Pi]/180, quarterAngle*\[Pi]/180],
getZ[halfAngle*\[Pi]/180, quarterAngle*\[Pi]/180]}]}],
Boxed -> False], {{quarterAngle, 0}, -90, 90}, {{halfAngle, 0}, -90,
90}]

```

## 5.2 Using the SPD

The lab's current SPD has a maximum intake of 22 MHz (photons per second). This requires attenuation of raw laser light.

Before using the SPD:

- Ensure that appropriate attenuation is in place before turning on the laser when the SPD is in its path.
- Do not attempt anything with the SPD until the alignment process has been completed (see Alignment>SPD).

To use the SPD:

1. The SPD must be connected to both a power source and the computer (via USB) to record data.
2. The GUI for the device is run on the lab computer. When first opening it up, the device must be selected: in the top left device>select device, click on the device or rescan for it, and hit connect.
3. Typically we use a Bin size of 100ms and record under “Free Running Timed Counter” mode.
4. Data is saved naturally as .txt files holding a 23 line header with mostly useless information and the bin count for each bin line by line. There is no need to alter these files; the python analysis programs handle it themselves. Simply save them as they are needed for your analysis program.

## 5.3 Setup

- Make sure the laser is being attenuated in either free space with neutral density filters or with a variable attenuator.
- Connect the attenuation to a fiber bench and connect the fiber bench to the SPD.
- Once all the components are in place, tape down the optic fibers with scotch tape and try not to move them during your experiments. The optic fibers change the polarization of the laser beam depending on how they are twisted and coiled.
- The first components in the fiberport will be for preparing a polarization state. Use just a polarizer for preparing linear polarizations or a polarizer and a quarter wave-plate for circular/elliptical polarization. The angles at which to set these components will depend on the characterization and maintenance of the components.

The measurement components needed and the order in which they should be placed depends on the type of QST being performed.

- For normal QST, place the quarter wave-plate after the preparation components and the polarizer after that for measuring circular/elliptical polarizations. Take out the quarter wave-plate for measuring linear polarizations.
- For SIC-POVM measurements, place the quarter wave-plate, then half wave-plate, then polarizer after the preparation components. If you don't need one or two of the wave-plates for measuring a certain state, take it out.

The angles at which you set these components will depend on characterization, maintenance, and most importantly the states you have chosen to form a tetrahedron inside the Bloch sphere. Always turn off the lights when recording QST data to minimize dark counts and for consistency.

#### 5.4 Mathematic Conventions and Conversions

- Instead of using the standard Bloch sphere, we used the Poincaré sphere for visualizing theoretical and measured polarization states.

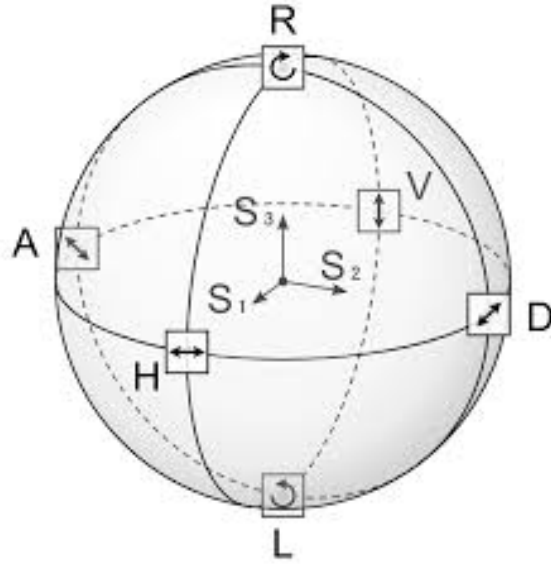


Figure 28: The Poincaré sphere.

- The  $\frac{\lambda}{4}$  ("quarter") wave-plate is represented by a counterclockwise turn on the Poincaré sphere.

Given a Bloch vector

$$|\psi\rangle = \begin{pmatrix} \alpha \\ \beta \end{pmatrix}, \quad (46)$$

to convert to  $x, y, z$  coordinates (or  $S_1, S_2, S_3$  Stokes parameters):

$$x = \alpha\beta^* + \alpha^*\beta, \quad (47)$$

$$y = i(\alpha^*\beta - \alpha\beta^*), \quad (48)$$

$$z = |\alpha|^2 - |\beta|^2. \quad (49)$$

Given  $x, y, z$  coordinates, to convert into a Bloch vector (up to a certain phase):

$$\theta = \cos^{-1}(z), \quad (50)$$

$$\phi = \tan^{-1}\left(\frac{y}{x}\right), \quad (51)$$

for the vector

$$|\psi\rangle = \cos(\theta/2)|0\rangle + e^{i\phi}\sin(\theta/2)|1\rangle. \quad (52)$$

## 5.5 Fidelity

The fidelity of a state (whether it be a density matrix or a pure state) is a measure of the “closeness” of two states. It expresses the probability that one state will pass a test to identify as the other. The fidelity of two density matrices is defined as:

$$F(\rho, \sigma) = \left( \text{Tr} \sqrt{\sqrt{\rho} \sigma \sqrt{\rho}} \right)^2. \quad (53)$$

If the state you’re comparing to is a pure state ( $\psi$ ) and the state you measured is a density matrix, then the fidelity reduces to:

$$F(\rho, \psi) = \langle \psi | \rho | \psi \rangle. \quad (54)$$

Lastly, if the states you’re comparing are both pure states, then the fidelity reduces again to

$$F(\phi, \psi) = |\langle \phi | \psi \rangle|^2. \quad (55)$$

Some authors also define the square root fidelity  $F' := \sqrt{F}$ .

## 5.6 Mystery Tomography

Perform quantum state tomography on an input state which is linearly polarized, but polarized at an unknown angle. Given the resulting density matrix, how can you determine the angle of the input polarizer? We can represent any pure state as

$$|\psi\rangle = \cos(\theta/2)|H\rangle + e^{i\phi}\sin(\theta/2)|V\rangle \quad (56)$$

Since we know the incoming light is linearly polarized, we know that  $\phi = 0$ . The density matrix of this input state is then

$$\rho = |\psi\rangle\langle\psi| = \begin{pmatrix} \cos^2(\theta/2) & \cos(\theta/2)\sin(\theta/2) \\ \cos(\theta/2)\sin(\theta/2) & \sin^2(\theta/2) \end{pmatrix}. \quad (57)$$

To retrieve the angle information from the density matrix state, we see that we can take the ratio of the bottom left corner of the matrix over the top left corner of the matrix to get  $\sin(\theta/2)/\cos(\theta/2)$ . We can then take the inverse tangent to solve for the angle:

$$\theta = 2 \arctan \left( \frac{\sin \theta/2}{\cos \theta/2} \right) = 2 \arctan \left( \frac{\rho_{10}}{\rho_{00}} \right). \quad (58)$$

Have one student prepare a mystery state while the other student performs QST on the state. Calculate the fidelity of the output state with respect to the input state and the percent error in the predicted angle. For a greater challenge, instead of only preparing input states which are linearly polarized, you will now prepare an arbitrary qubit state. This can be done by placing a  $\lambda/2$  and  $\lambda/4$  waveplate after linearly polarizing the input. If the first polarizer is placed in the  $|H\rangle$  state, then the resulting input state  $|\psi\rangle$  can be calculated:

$$|\psi\rangle = W_Q(\theta_Q)W_H(\theta_H)|H\rangle \quad (59)$$

Using the predicted input state, calculate the fidelity after performing QST.

## 5.7 Maximum Likelihood Estimation

Physical states are represented by density matrices that are normalized, Hermitian, and positive. To ensure these three properties hold, we will create our density matrix from a lower triangular matrix  $T$ , as  $\rho = T^\dagger T$ . This matrix satisfies the three necessary properties:

- (i) *Non-negative*: To satisfy non-negativity, the probability of an arbitrary state must be non-negative, i.e.  $\langle \psi | \rho | \psi \rangle \geq 0$ . For our density matrix,  $\langle \psi | T^\dagger T | \psi \rangle = \langle \psi' | \psi' \rangle \geq 0$ .
- (ii) *Hermitian*: This construction of the density matrix is Hermitian:  $\rho^\dagger = (T^\dagger T)^\dagger = T^\dagger T = \rho$ .

(iii) *Normalized*: Normalization can be ensured by dividing by the trace:

$$\rho = \frac{T^\dagger T}{\text{Tr}[T^\dagger T]}.$$

The  $T$  matrix must be hermitian and contain the necessary degrees of freedom to satisfy any real density matrix. Such a matrix is:

$$T(t_1, t_2, t_3, t_4) = \begin{pmatrix} t_1 & 0 \\ t_2 + it_3 & t_4 \end{pmatrix}. \quad (60)$$

For brevity, we will write the  $(t_1, t_2, t_3, t_4)$  parameters as a vector  $\vec{t}$ . The resulting density matrix as a function of the free parameters is

$$\rho(\vec{t}) = \frac{T^\dagger(\vec{t})T(\vec{t})}{\text{Tr}[T^\dagger(\vec{t})T(\vec{t})]}. \quad (61)$$

The elements  $\vec{t}$  must be found during optimization. We can assume that the number of counts coming into the photon detection is distributed along a Poisson distribution, for which we care about the mean. Due to the central limit theorem, the mean of this Poisson distribution follows a Gaussian. The probability to obtain a set of  $\{n_j\}$  counts, where  $n_j$  is the average number of counts per bin and  $j$  ranges over each basis measurement, is

$$P(\{n_j\}) = \frac{1}{\alpha} \prod_j \exp \left[ -\frac{(n_j - \bar{n}_j)^2}{2\sigma_j^2} \right], \quad (62)$$

where  $\alpha$  is a normalization constant for each of the Gaussian distributions,  $\bar{n}_j$  is the parent population mean for each Gaussian, and  $\sigma_j$  is the parent standard deviation for the  $j$ th record, which can be approximated by  $\sqrt{\bar{n}_j}$ . The expected counts are connected to the state described by

$$\bar{n}_j(\vec{t}) = N \langle \psi_j | \rho(\vec{t}) | \psi_j \rangle, \quad (63)$$

with  $N$  being the total number of counts(for that basis measurement  $j$ ). The full expression for the probability is

$$P(\{n_j\}) = \frac{1}{\alpha} \prod_j \exp \left[ -\frac{(N \langle \psi_j | \rho(\vec{t}) | \psi_j \rangle - n_j)^2}{2N \langle \psi_j | \rho(\vec{t}) | \psi_j \rangle} \right]. \quad (64)$$

The maximum likelihood for our parameters  $\vec{t}$  are then given by the maximum of this function. Numerically we can drop the constant  $\alpha$ , and we can also take the logarithm of the function because the logarithm is a monotonically increasing function. Lastly, since it is easier to minimize functions in Python, we can find the minimum of the negative of equation (64), which is:

$$L(\vec{t}) = \sum_j \frac{(N \langle \psi_j | \rho(\vec{t}) | \psi_j \rangle - n_j)^2}{2N \langle \psi_j | \rho(\vec{t}) | \psi_j \rangle}. \quad (65)$$

This function is called the likelihood function, or more specifically the log-likelihood function. The programmatic implementation is a multivariate optimization problem in terms of the components  $\vec{t}$ .

## 5.8 Error Analysis

- Taylor Series Expansion Error Propagation

We first determined our values of error by Taylor series expansion error propagation. Consider a function of our measured counts' Taylor expansion where the terms of the expansion use theoretical counts:

$$f(\hat{\lambda}) = \sum_{n=0}^{\infty} \frac{f^{(n)}(\lambda)}{n!} \epsilon^n$$

$$f(\hat{\lambda}) = f(\lambda) + f'(\lambda)\epsilon + \frac{f''(\lambda)}{2!}\epsilon^2 + \dots$$

In this method of error analysis  $\epsilon^2$  is considered to be much smaller than  $\epsilon$  and is negligible:

$$\epsilon^2 \ll \epsilon$$

However, since our distribution is Poissonian, the value  $\epsilon$  is very close to the average photon count:

$$\epsilon \approx \lambda$$

Therefore,  $\epsilon^2$  is not much smaller than  $\epsilon$ , is not negligible, and another method of error analysis must be used.

- Bounded Confidence Interval

The measured counts ( $\hat{\lambda}$ ) can be set equal to the theoretical counts ( $\lambda$ ) plus the theoretical errors ( $\epsilon$ ):

$$\begin{aligned}\hat{\lambda}_H &= \lambda_H + \lambda_{DC} + \epsilon_H \\ \hat{\lambda}_V &= \lambda_V + \lambda_{DC} + \epsilon_V \\ \hat{\lambda}_{DC} &= \lambda_{DC} + \epsilon_{DC}\end{aligned}$$

The 95% confidence interval for the theoretical errors are bounded by  $\eta = f(\hat{\lambda})$ :

$$\begin{aligned}|\epsilon_H| &\leq \eta_H \\ |\epsilon_V| &\leq \eta_V \\ |\epsilon|_{DC} &\leq \eta_{DC}\end{aligned}$$

The theoretical probability of the photons having a certain state subtracted from the measured probability is equal to the total error:

$$\hat{z} - z = \epsilon = \frac{\hat{\lambda}_H - \hat{\lambda}_{DC}}{\hat{\lambda}_H + \hat{\lambda}_V - \hat{\lambda}_{DC}} - \frac{\lambda_H}{\lambda_H + \lambda_V}$$

Algebraic manipulations of the above equations and inequalities can yield a total error that is a function of only theoretical values and is therefore more accurate:

$$\begin{aligned}(\hat{\lambda}_H + \hat{\lambda}_V - 2\hat{\lambda}_{DC}) &= \lambda_H + \lambda_V + \epsilon_H + \epsilon_V - 2\eta_{DC} \\ \hat{\lambda}_H - \hat{\lambda}_{DC} &= \lambda_H + \epsilon_H - \epsilon_{DC} \\ (\lambda_H + \lambda_V)(\lambda_H + \lambda_V + \epsilon_H + \epsilon_V - 2\epsilon_{DC})\epsilon &= (\lambda_H + \epsilon_H - \epsilon_{DC})(\lambda_H + \lambda_V) - \lambda_H(\lambda_H + \lambda_V + \epsilon_H + \epsilon_V - 2\epsilon_{DC}) \\ &= (\epsilon_H - \epsilon_{DC})(\lambda_H + \lambda_V) - \lambda_H(\epsilon_H + \epsilon_V - 2\epsilon_{DC}) \\ &= -\epsilon_{DC}(\lambda_H + \lambda_V) + \epsilon_H \lambda_V - \lambda_H(\epsilon_V - 2\epsilon_{DC}) \\ &\leq -\epsilon_{DC}(\hat{\lambda}_H - \eta_H + \hat{\lambda}_V - \eta_V) + \epsilon_H(\hat{\lambda}_V + \eta_V) - (\hat{\lambda}_H \pm \eta_H)(\epsilon_V - 2\epsilon_{DC}) \\ \epsilon &= \frac{-\epsilon_{DC}(\lambda_H + \lambda_V) + \epsilon_H \lambda_V - \lambda_H(\epsilon_V - \epsilon_{DC})}{(\lambda_H + \lambda_V)(\lambda_H + \lambda_V + \epsilon_H + \epsilon_V - 2\epsilon_{DC})}\end{aligned}$$

- Bounded Confidence Interval for a Poisson Distribution

The most successful and accurate error analysis method we used was a bounded confidence interval for a Poisson Distribution. The probability that the error will be bounded by some  $\eta$  is at least 95%:

$$Pr[|\epsilon| \leq \eta] \geq 95\%$$

Where  $\eta$  is a function of the average photon counts and the number of bins:

$$\eta = 1.96 \sqrt{\frac{\lambda}{n}}$$

Thus, the 95% confidence interval is:

$$\hat{\lambda} \pm 1.96 \sqrt{\frac{\hat{\lambda}}{n}}$$

## 5.9 Python Programs

- **Jun26QstFunctions.py** performs standard QST, using 6 measurements to find the expectation value of the Pauli X, Y, and Z matrices. It is mostly outdated, and no other program makes reference to it. It is entirely replicated by Jul13QstFunctions.py
- **SICPOVM.py** performs SIC-POVM QST and is similar to the previous one in that it is outdated. It can be used by calling it from a program in the folder of the data.
- **Jul13QstFunctions.py** contains generalized functions used by the main tomography programs (tomography.py and stdTomo.py) including the error calculation functions (ei and getEtas), data file reading/processing function called getMeanVar (with the getAvgMeanVar variant), fidelity (with the fidFromDmats variant), and smush. This program also has a main function which can be called by a program in the same folder as the data to be analyzed. Main takes an expected state to be used for fidelity calculation.
- **angleCalc.py** contains methods for converting between states and wave-plate angles and vice versa. The program itself is well commented and requires no further documentation.
- **Automated SIC POVM Tomography**
  - **QST.ahk** is an automation script for performing SIC-POVM QST. While holding the ‘q’ and ‘s’ key, press ‘t’ to begin the script which will prompt you for a folder name to hold your data. The script will only behave as intended if the following conditions are met:
    - \* The Thorlabs SPC GUI is running and the proper SPC device has been connected.
    - \* Anaconda Prompt is open to Desktop\Experiments\Programs.
    - \* Kinesis is fully booted up.
  - **Tomography.py** performs all of the calculations during the automated SIC-POVM QST. It takes one command line argument which is supposed to be the path of the folder containing the data. It writes the quarter and half wave-plate angles corresponding to a SIC-POVM set of measurements to a file in Programs called runData.txt, which is read by the autohotkey program. It then waits as the data is collected before making the tomography calculation, printing the results to the console, and displaying the results graphically using Bloch.py. You can run this program without the automated step if the data has already been collected. After printing to the console, the program also writes to a log file in the same folder as the data called result.txt. The program currently displays a fidelity but this is only used if you know the state you are preparing which must be communicated to the program manually.
- **Automated Standard Tomography**
  - **std.ahk** is the standard QST analogue to QST.ahk. It behaves the exact same way
  - **stdTomo.py** is the standard QST analogue to tomography.py. It behaves the exact same way.

- **Graphing scripts**

- **Bloch.py** uses matplotlib to graph stokes vectors on the Poincaré sphere. The stokesToVector function graphs a stokes vector in the sphere. The diffVector function is used to show a vector point from the tip of an expected state vector to the tip of a measured state vector, or more generally a vector between the tips of two vectors. After drawing all the wanted vectors, use show() to make the graph appear when the program is run; make sure to do this last.
- **PhiVThetaPlotter.py** reads one or two data files ("expectedData.txt" and "measuredData.txt" in the directory of the 'path' variable) containing theta and phi, corresponding to spherical coordinate for a sequence of observed states. It scatter plots the data with phi on the horizontal axis and theta on the vertical axis. These files ought to be
- **graphQuarterFamily.py**, **graphQMixedFamily.py**, **AnalyzeLaser.py** parse data from particular experiments and prepare it to be plotted. Also set up for Bloch Sphere graphing. Could be used as a template for further data analysis programs. Each reads the result.txt files generated by each tomography.py and generates expectedData.txt and/or measuredData.txt.

- **Misc.**

- **FirstScript.ahk** creates a message box displaying the screen-mode x and y coordinates of the cursor when the hotkey Ctrl+G is used. Useful for writing other autohotkey programs.
- **Jun27-Waveplate-Char.py** was used to plot data from an experiment characterizing one of the half waveplates in the lab. The only use now is to show examples of how to use matplotlib for similar purposes.

For the use of any QST program, data files ought to be named a number 0 through 3 for SIC-POVM or a single lowercase letter corresponding to the pure state measured (e.g. h, d, or r) for standard QST. The automation scripts do this properly already. Save the data files as .txt files.

## 5.10 Tomography using the Qubit SIC-POVM

This is a form of QST using a special set of nonorthogonal bases of measurement. It is useful because, in higher dimensions than that of our single qubit, use of such measurement bases is more “efficient.” In a single qubit, the proper set of states forms a regular tetrahedron in the Bloch sphere.

Consider a set of four pure polarization states that form a tetrahedron in the Bloch sphere:

$$|\psi_0\rangle, |\psi_1\rangle, |\psi_2\rangle, |\psi_3\rangle$$

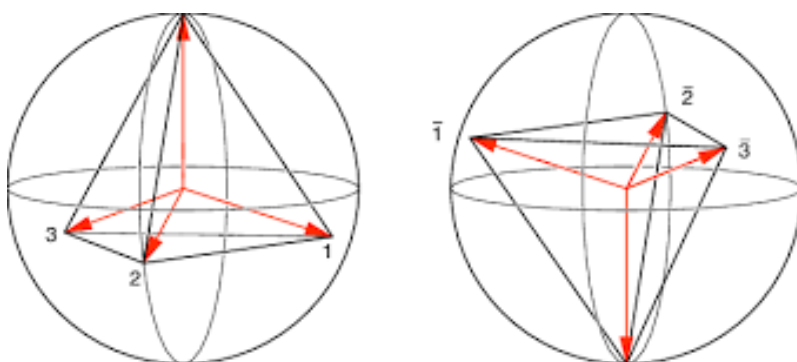


Figure 29: These are two possible Bloch vector sets for SIC-POVM. There are infinite tetrahedron-forming Bloch vector sets for performing SIC-POVM.

Consider the inner product of any two kets in the above set (the kets can be either identical or different):

$$\langle \psi_i \rangle \psi_j$$

When  $i = j$ :

$$\langle \psi_i \rangle \psi_j = 1$$

When  $i \neq j$ :

$$\langle \psi_i \rangle \psi_j = \frac{1}{4}$$

The probability of measuring a certain state from the tetrahedron set is equal to the trace of the product of the density matrix of the unknown state being measured and the outer product of the certain state from the tetrahedron set:

$$Pr(|\psi_i\rangle) = Tr[\rho |\psi_i\rangle\langle\psi_i|]$$

A vector containing the probabilities of measuring the tetrahedron states can be set equal to the product of a matrix containing the Stokes parameters of the tetrahedron states, a vector containing the Stokes parameters of the unknown state, and some constant:

$$\underbrace{\begin{bmatrix} Pr(\psi_0) \\ Pr(\psi_1) \\ Pr(\psi_2) \\ Pr(\psi_3) \end{bmatrix}}_{\hat{P}} = \underbrace{\begin{bmatrix} 1 & r_{0,X} & r_{0,Y} & r_{0,Z} \\ 1 & r_{1,X} & r_{1,Y} & r_{1,Z} \\ 1 & r_{2,X} & r_{2,Y} & r_{2,Z} \\ 1 & r_{3,X} & r_{3,Y} & r_{3,Z} \end{bmatrix}}_{\hat{M}} \underbrace{\begin{bmatrix} 1 \\ v_X \\ v_Y \\ v_Z \end{bmatrix}}_{\hat{V}} C$$

$$\hat{P} = \hat{M} \cdot \hat{V}$$

Using measured values for  $\hat{P}$  and known values of  $\hat{M}$  (since we can choose these four states as long as they form a tetrahedron), we can solve for  $\hat{V}$ , thereby accomplishing a state reconstruction (QST):

$$\hat{V} = \hat{P} \hat{M}^{-1} \frac{1}{C}$$

The SIC-POVM QST process goes as follows:

1. Choose four states and calculate their stokes parameters for  $\hat{M}$ . It will save time and stress to choose one state that is easy to prepare and calculate, then use geometry and trigonometry to calculate the others.
2. Determine how to measure from the tetrahedron states using optical components.
3. Record the photon count for the overall signal (no measurement components) and for each state individually.
4. The probabilities for  $\hat{P}$  of measuring any of the tetrahedral states are given by the ratio of counts in the measured state to the signal (after adjusting for dark counts).

Here is an example set of tetrahedral states:

| Vector           | $x$   | $y$   | $z$   | $\theta_Q$  | $\theta_H$     |
|------------------|-------|-------|-------|-------------|----------------|
| $ \psi_0\rangle$ | 0     | 1     | 0     | $0^\circ$   | $-22.5^\circ$  |
| $ \psi_1\rangle$ | 0     | -0.33 | 0.94  | $0^\circ$   | $4.875^\circ$  |
| $ \psi_2\rangle$ | 0.81  | -0.33 | -0.47 | $60^\circ$  | $34.875^\circ$ |
| $ \psi_3\rangle$ | -0.81 | -0.33 | -0.47 | $-60^\circ$ | $64.875^\circ$ |

## 5.11 6 vs 4 measurements

Typically in QST, we measure both  $|H\rangle$  and  $|V\rangle$  to attain the expectation value of the observable  $Z$ , implying a total of 6 measurements (2 for each of the three observables).

However, since we know:

$$P(\phi) + P(\phi_{\perp}) = 1$$

and all of the Pauli observables have orthogonal eigenvectors, the expectation of any of the Pauli observables can be calculated with only one measurement each.

Standard QST only requires three measurements for the three observables and one extra for the signal. Our current data suggests that 4 measurement standard QST is negligibly worse than 6 measurement standard QST. Our SIC-POVM measurements were conducted in this way: 4 measurements for the four tetrahedral states, without measuring the states' orthonormal partners. SIC-POVM, as it turns out, does not require a measurement of signal since it is multiplied into a scalar coefficient of the matrix equation.

## 5.12 Mixed State Preparation and QST

For a basic run of mixed state QST:

1. After aligning the 3-sided fiber bench with the beam splitter, connect two lasers to the 3-sided fiber bench so that they combine and travel to a fiber bench for QST measurement.
  2. Perform QST on both lasers individually, then combined. The individual lasers should have approximately orthogonal polarizations.
  3. Once the density matrix and/or Bloch vector for the mixed state is calculated, check it by manually combining the density matrices of the individual laser QST's.
- The diagram under section 4.9 displays a mixed state QST set up with automated measurement components instead of a fiber bench.
  - Any form of QST can be used, just be consistent.

## 5.13 Automated QST

The objective of our automated QST experiments is to create an optical setup and series of programs that can essentially run QST by itself. The only manual tasks should be turning the laser, the APD and the stepper motors on and clicking one button that starts the entire sequence.

**Note:** Our automated QST is not nearly as accurate as when we rotated the polarizers and wave-plates by hand in a single fiber bench. Automated QST fidelities are usually about  $.85 \pm .05$  while our manual fidelities were always  $.9$  and higher, very close to 1.

- To measure certain states (the task in QST that usually requires a person to manually rotate the measurement components), stepper motors will rotate quarter and half wave-plates and a final polarizer is placed after these motors at a constant angle.
- Note: The line for horizontal on the motors is different than the one on the wave-plates. Determine this offset and account for it when determining what angles the wave-plates should be rotated to.
- In theory, an advantage of automated stepper motors is their rotation accuracy relative to "eyeballing it". However, in practice one or both motors turns too far or doesn't turn at all due to a poor USB connection.
- Programs needed include an Auto Hot Key sequence, Kinesis software, the SPD software, and the Python programs for data analysis and 3-D graphing of the Bloch vector.

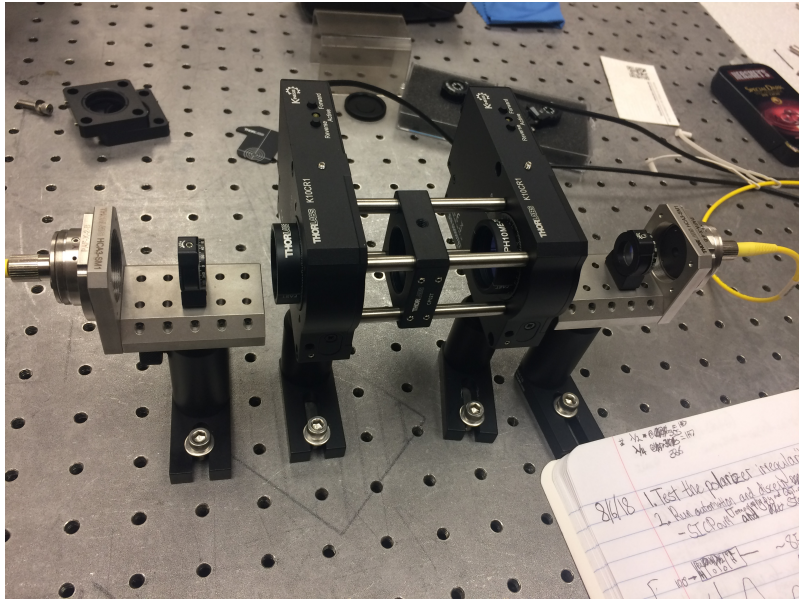


Figure 30: These are the components used in our automated QST. before them, the laser is attenuated by a variable attenuator and after them is the SPD. From left to right: FiberPort collimator, preparation polarizer (P1), stepper motor with quarter wave-plate, stepper motor with half wave-plate, measurement polarizer (P2), FiberPort collimator.

To construct the automatic measurement apparatus:

1. Take the second collimator off of the preparation FiberPort and put it on the end of another FiberPort that has the first collimator removed. Make sure the two collimators being used are the same model.
2. Put the free space quarter and half wave-plates in two stepper motors. Connect the motors via the "cage" metal bars.
3. Mount the motors as shown above, at a relatively short height.
4. Mount the FiberPorts at a slightly higher height so that the laser will go through the center of the wave-plates and be aligned with the two collimators. It may be helpful to have the laser turned on and unattenuated and the apparatus connected to the power meter while mounting before screwing everything into place to be sure that all components are at the correct height and are in line with each other.
5. Fine tune the alignment using the power meter as if aligning a single two-sided FiberPort.

#### Pure States Experiment:

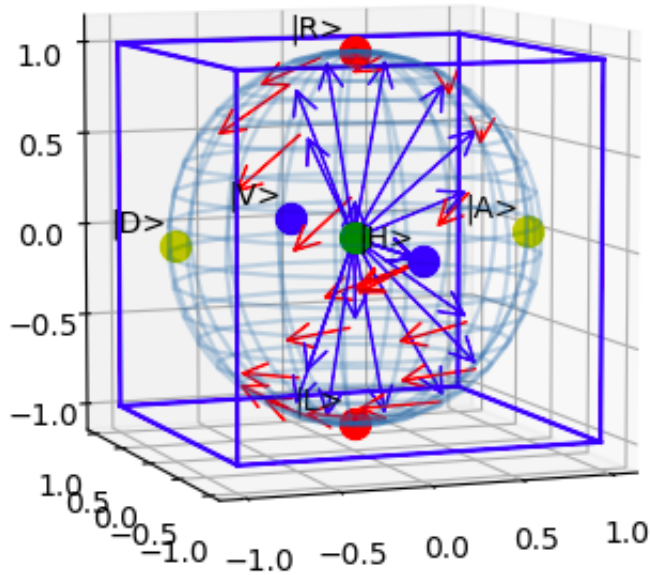


Figure 31: Blue: Measured States. Red: Expected States.

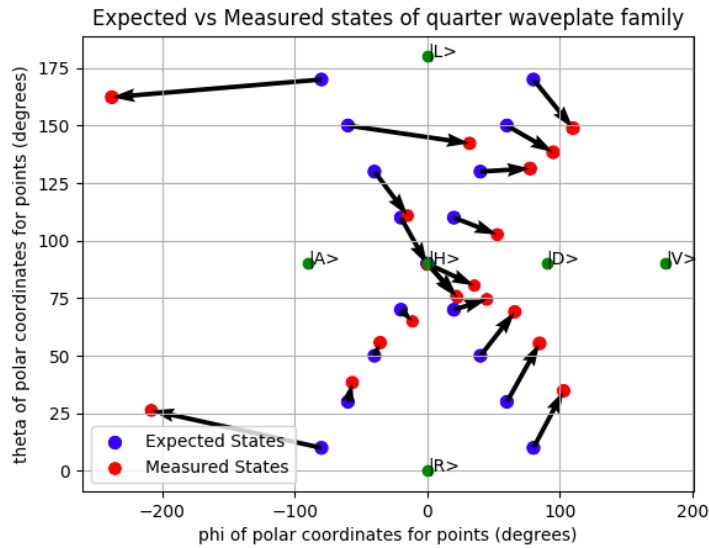


Figure 32: 2D Representation of expected vs measured states.

#### Systematic Error Experiment:

To gauge the error in our system unattributable to minor variations in the performance of our lab equipment, we conducted two experiments. First, tomography of the laser, altered only by passing through necessary fibers, using randomly generated SIC tetrahedrons for POVM. We then conducted the same experiment on a prepared state,  $|H\rangle$ . The following two graphs display the resulting measured states on  $\phi$  vs.  $\theta$  plots of their spherical coordinates.

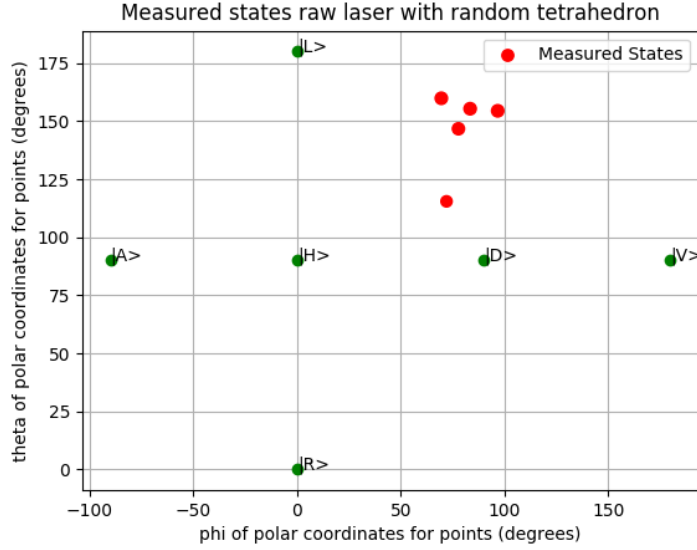


Figure 33: The observed states from measuring the same state, namely the unfiltered laser, with 5 randomly rotated regular tetrahedrons. The laser does pass through two fibers, meaning two unknown unitary transformations have been applied. The  $(X, Y, Z)$  Bloch vectors had mean  $(0.377, -0.877, 0.061)$  with standard deviations  $(0.056, 0.069, 0.068)$  and mean length 0.960 with standard deviation 0.075

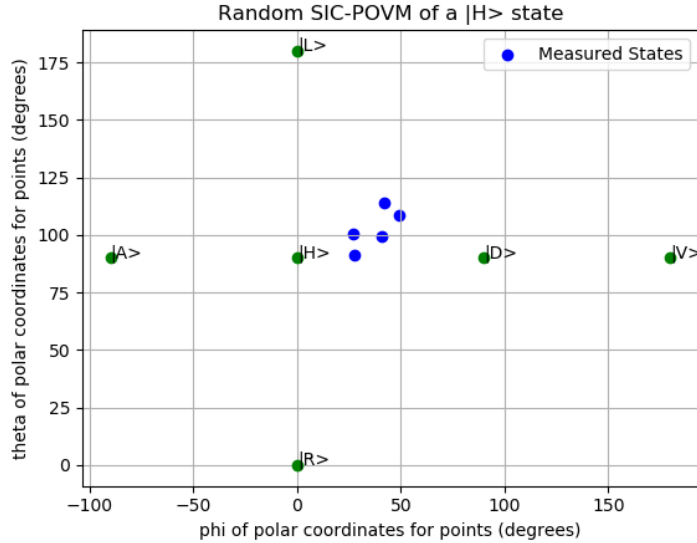


Figure 34: The observed states from measuring the same prepared state, namely  $|H\rangle$ , with 5 randomly rotated regular tetrahedrons. The  $(X, Y, Z)$  Bloch vectors had mean  $(0.518, -0.302, 0.703)$  with standard deviations  $(0.064, 0.202, 0.179)$  and mean length 0.956 with standard deviation 0.061. The mean fidelity of the measured states with respect to horizontal is 0.852 with a standard deviation of 0.089.

Although the measurement of states is shown to vary as the orientation of the tetrahedron varies, the variation is not significant enough to reach the expected  $|H\rangle$  state. The fidelity, though, can reach satisfactory levels. The graphs demonstrate that the skew is generally in the same direction. According to our notes, this "walk" of the measured state appears to have been introduced along with the setup for automated QST. Before automation, we generally reached fidelities above 0.95 and frequently with at least two 9's. The data for those results are on the github repository (in the June and July folders), but the results themselves were only ever recorded by hand.

## 5.14 Mixed State Automated QST

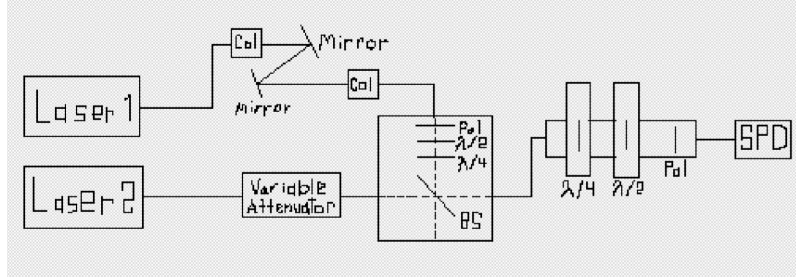


Figure 35: This is a mixed state, automated QST set up. The boxes enclosing the last two wave-plates are stepper motors.

The light from Laser 1 is prepared as  $|\psi\rangle$  and the light from Laser 2 is highly polarized and can be represented by the density matrix  $\rho_l$ . After the beams are combined by the beam splitter, the resulting density matrix should be:

$$\rho = p |\psi\rangle \langle \psi| + (1 - p)\rho_l$$

"p" for each laser is the probability of that laser's density matrix being measured as the resultant density matrix. This probability is proportional to their relative intensities.

### Mixed States Automated QST Experiment:

Our raw laser light ( $\rho_l$ ) is roughly a pure state. The prepared state ( $|\psi\rangle$ ) started as horizontal, with a polarizer rotated to the horizontal position and a quarter wave-plate at  $0^\circ$ . The intensities of the two lasers were as identical as possible. After this, the prepared state was altered by turning the quarter wave-plate in  $10^\circ$  increments through  $180^\circ$ .

Graphing the results:

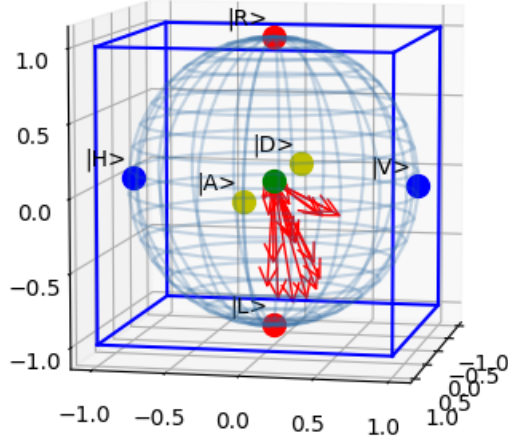


Figure 36: The red vectors in the above 3-D Poincaré graph are our measured Bloch vectors for each  $10^\circ$  iterative rotation of the quarter wave-plate.

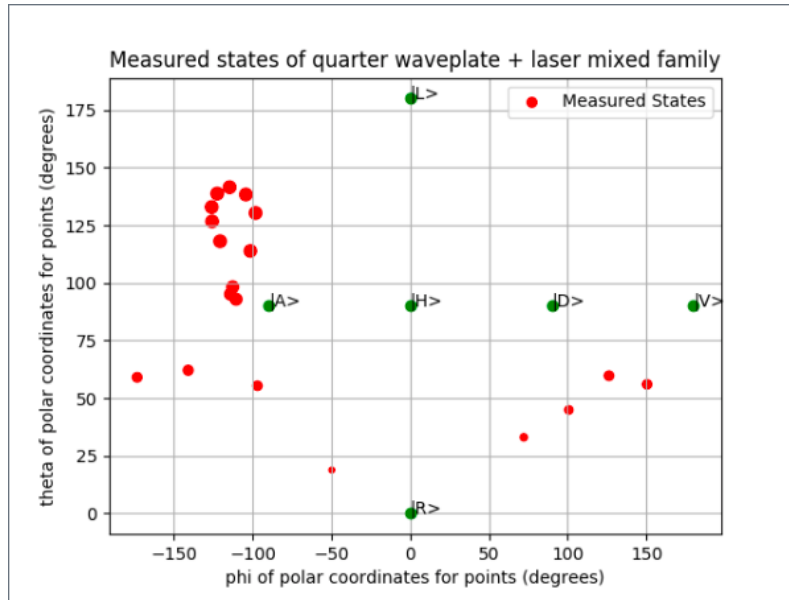


Figure 37: The same data represented in spherical coordinates. The size of the marker correlates to the radius of the point.

- Graphically, our results roughly follow the theoretical figure 8 pattern rotations of a quarter wave-plate map on the Bloch and Poincaré spheres
- While the measured vectors had relatively high fidelities, the errors are all trending in the same direction. This suggests some sort of systematic error in our optical set up.

## References

- [1] Agarwal, Girish S. *Quantum Optics*. Cambridge University Press, 2015.
- [2] Bachor, Hans-Albert. *A Guide to Experiments in Quantum Optics*. Wiley-VCH, 1998.
- [3] Guenther, Robert D. *Modern Optics*. John Wiley, 1990.
- [4] Kwiat, Paul G. "Guide to Quantum State Tomography." *Kwiat Quantum Information Group*. 2018, research.physics.illinois.edu/QI/Photonics/Tomography/.
- [5] Bayraktar, Omer "Quantum-Polarization State Tomography." <http://www.diva-portal.org/smash/get/diva2:923925/FULLTEXT02.pdf>
- [6] Thorlabs. "User Guide." Thorlabs, www.thorlabs.com/drawings/6a798f07a3cb2a5e-A0B0559D-FA03-5001-3C8B771E9B8D4539/PAF-X-5-B-Manual.pdf
- [7] PHY 315L - Waves and Optics Lab *Polarization course material*